



**HAL**  
open science

## Interpreting discrepancies between discharge and precipitation in high-altitude area of Chile's Norte Chico region (26–32°S)

Vincent Favier, Mark Falvey, Antoine Rabatel, Estelle Praderio, David López

### ► To cite this version:

Vincent Favier, Mark Falvey, Antoine Rabatel, Estelle Praderio, David López. Interpreting discrepancies between discharge and precipitation in high-altitude area of Chile's Norte Chico region (26–32°S). *Water Resources Research*, 2009, 45, pp.W02424. 10.1029/2008WR006802 . insu-00420411

**HAL Id: insu-00420411**

**<https://insu.hal.science/insu-00420411>**

Submitted on 10 Mar 2021

**HAL** is a multi-disciplinary open access archive for the deposit and dissemination of scientific research documents, whether they are published or not. The documents may come from teaching and research institutions in France or abroad, or from public or private research centers.

L'archive ouverte pluridisciplinaire **HAL**, est destinée au dépôt et à la diffusion de documents scientifiques de niveau recherche, publiés ou non, émanant des établissements d'enseignement et de recherche français ou étrangers, des laboratoires publics ou privés.

## Interpreting discrepancies between discharge and precipitation in high-altitude area of Chile's Norte Chico region (26–32°S)

Vincent Favier,<sup>1,2</sup> Mark Falvey,<sup>3</sup> Antoine Rabatel,<sup>1</sup> Estelle Praderio,<sup>1,4</sup> and David López<sup>1</sup>

Received 2 January 2008; revised 4 July 2008; accepted 4 November 2008; published 19 February 2009.

[1] The water resources of high-altitude areas of Chile's semiarid Norte Chico region (26–32°S) are studied using surface hydrological observations (from 59 rain gauges and 38 hydrological stations), remotely sensed data, and output from atmospheric prediction models. At high elevations, the observed discharge is very high in comparison with precipitation. Runoff coefficients exceed 100% in many of the highest watersheds. A glacier inventory performed with aerial photographs and ASTER images was combined with information from past studies, suggesting that glacier retreat could contribute between 5% and 10% of the discharge at 3000 m in the most glacierized catchment of the region. Snow extent was studied using MOD10A2 data. Results show that snow is present during 4 months at above 3000 m, suggesting that snow processes are crucial. The mean annual sublimation ( $\sim 80 \text{ mm a}^{-1}$  at 4000 m) was estimated from the regional circulation model (WRF) and data from past studies. Finally, spatial distribution of precipitation was derived from available surface data and the global forecast system (GFS) atmospheric prediction model. Results suggest that annual precipitation is three to five times higher near the peak of the Andes than in the lowlands to the west. The GFS model suggests that daily precipitation rates in the mountains are similar to those in the coastal region, but precipitation events are more frequent and tend to last longer. Underestimation of summer precipitation may also explain part of the excess in discharge. Simple calculations show that consideration of GFS precipitation distributions, sublimation, and glacier melt leads to a better hydrological balance.

**Citation:** Favier, V., M. Falvey, A. Rabatel, E. Praderio, and D. López (2009), Interpreting discrepancies between discharge and precipitation in high-altitude area of Chile's Norte Chico region (26–32°S), *Water Resour. Res.*, 45, W02424, doi:10.1029/2008WR006802.

### 1. Introduction

[2] In the context of a rapidly changing climate, the estimation and modeling of water resources is a central issue for sustainable development in arid environments [e.g., *Intergovernmental Panel on Climate Change (IPCC)*, 2007]. It is especially relevant in the semiarid Norte Chico region of Chile (from 26°S to 32°S; Figure 1) where climate variability over the 20th century has been characterized by decreasing precipitation [*Santibañez*, 1997; *Le Quesne et al.*, 2006; *Vuille and Milana*, 2007] and aridification [*Squeo et al.*, 2007]. Most of the regions water resources originate in the Andes cordillera (mountain range), either from direct runoff during winter rainstorms or from snowmelt during spring and early summer. Despite their profound importance to local agriculture (a major part of the local economy), both precipitation and discharge are poorly observed in the Andes, especially at high elevations (i.e., >3000 m above sea level (asl)), which are often inaccessible and covered by snow

during winter. Glacier coverage in Norte Chico region is small (73.85 km<sup>2</sup> [*Garin*, 1987; *Rivera et al.*, 2000]), but the substantial retreat of glaciers during the 20th century [e.g., *Leiva*, 1999; *Rivera et al.*, 2002] is generally assumed to play a significant role in discharge variations. Except for rough estimations of water contribution from the cryosphere [*Rivera et al.*, 2002], little data are available to clearly infer the impact of glacier retreat on discharge in the area. Information on snow accumulation (rutas de nieve from Dirección General de Agua (DGA) [*Escobar and Aceituno*, 1998]) and sublimation/evaporation [*Stichler et al.*, 2001; *Ginot et al.*, 2006] is even scarcer, and the spatial distribution of hydrological measurements is insufficient to correctly infer the spatial distribution of water production. As such, a basic understanding of hydrological processes in the Andean catchments of the Norte Chico is lacking.

[3] The objective of this study is to provide a careful characterization of the hydrological regime of the Andes of the Norte Chico Region, focusing on high-altitude areas above 3000 m asl. Given that the region is effectively unstudied (from a hydrological perspective), our approach is largely empirical and we place substantial emphasis on the presentation and interpretation of available observational data. We examine several aspects of the hydrological regime, including long term variability of precipitation and discharge over the 20th century, spatial and temporal

<sup>1</sup>Laboratorio de Glaciología, CEAZA, La Serena, Chile.

<sup>2</sup>Laboratoire de Glaciologie et de Géophysique de l'Environnement, Saint Martin d'Hères Cedex, France.

<sup>3</sup>Departamento de Geofísica, Universidad de Chile, Santiago, Chile.

<sup>4</sup>Division Hydraulique de Rivière, Hydrétudes, Argonay, France.

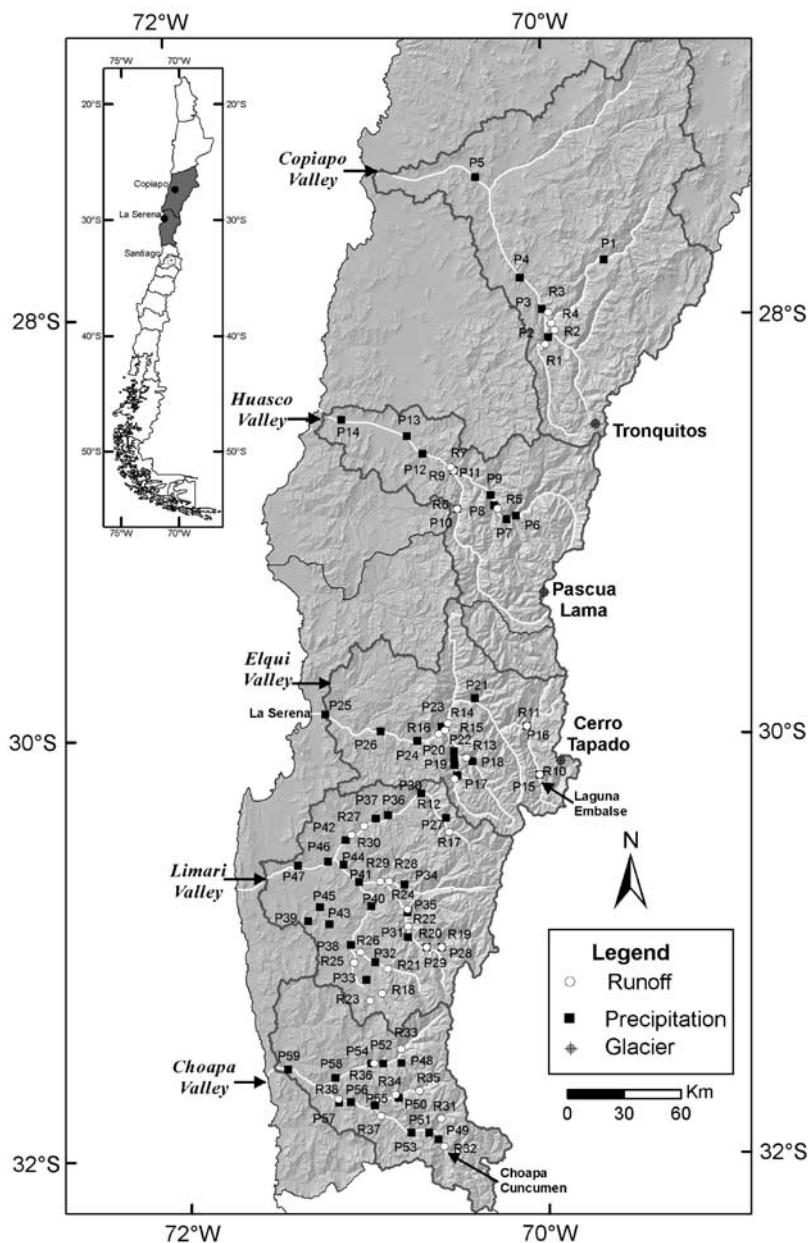


**Figure 1.** Map of Norte Chico region showing the runoff stations (white points), rain gauges (black squares), and main glaciers (gray circles). Names and characteristics of the stations are defined in Tables 1 and 2.

patterns of snow cover, and the region's glaciers. An important goal of our study is to understand the water contribution from high-altitude areas of the Andes (>3000 m asl). This goal is motivated by the fact that many of the river gauge stations at the outlets of the highest catchments show significant runoff excess when compared to available precipitation data. We pay particular attention to possible water contributions due to glacial retreat, orographic precipitation enhancement, and water losses due to sublimation. To compensate for the lack of traditional data at high altitudes we review field observations presented in past literature and use remotely sensed data to evaluate snow and glacier cover. In addition, atmospheric models (global and regional) are employed to provide further insight into poorly measured processes such as precipitation and sublimation. Our results

are used in simple water budget calculations that demonstrate how inclusion of estimates of glacial retreat, sublimation and orographic precipitation enhancement can better explain observed river discharges. We trust that the results presented herein will provide a sound basis for future studies incorporating more sophisticated hydrological modeling approaches.

[4] The paper is organized as follows. After a description of the regional climatic conditions and variability (section 2), we describe the data and methods used in section 3. In section 4, we examine the long term variability of precipitation and discharge during the 20th century at low and high altitudes. In section 5, precipitation and discharge are compared. In section 6 we examine the hydrological characteristics of the high-altitude catchments in more detail,

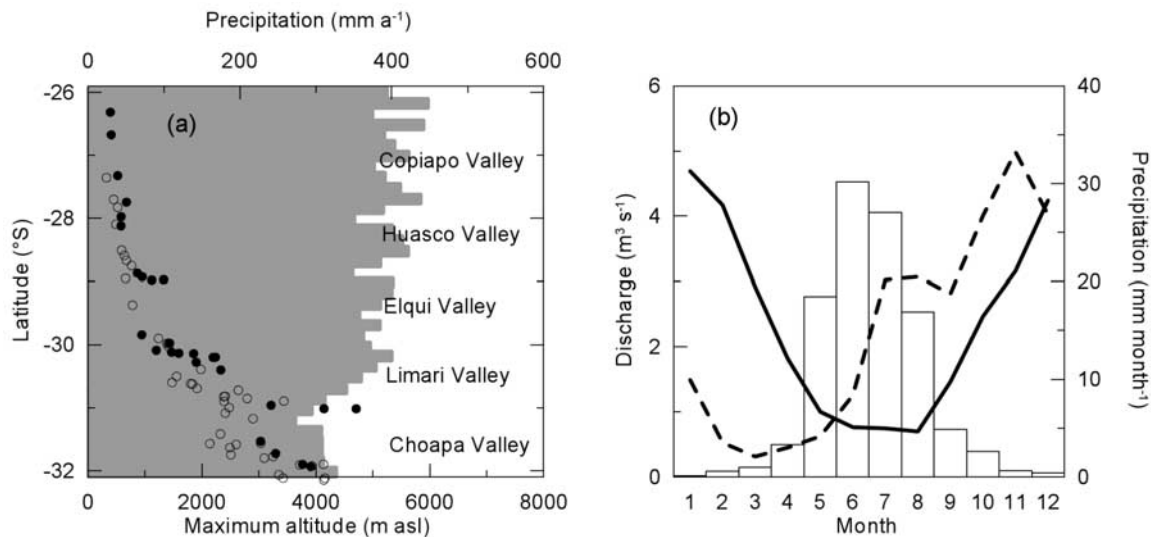


**Figure 2.** (a) Evolution of precipitation with latitude. Open circles are annual mean precipitation at sites lower than 750 m asl; filled circles reflect precipitation at sites higher than 750 m asl. Gray horizontal bars indicate the maximum altitude of the Andes at 0.16° intervals. (b) Seasonal variation of precipitation and discharge in Norte Chico region. The open bars are mean monthly precipitation between 1900 and 2005 at La Serena-La Florida airport (P25 in Figure 1, 29°54'S, 71°12'W, 142 m asl). The continuous line is mean monthly discharge at La Laguna Embalse station (R10 in Figure 1, 30°12'S, 70°02'W, 3130 m asl) between 1964 and 2005. The dashed line is monthly discharge of Hurtado River at Recoleta Dam (R30, 30°28'S, 71°04'W, 410 m asl) between 1928 and 1984.

including an evaluation of glacial cover and the contribution of glacial retreat to river discharges (section 6.1), description of the spatial and temporal variability of snow cover (section 6.2), the evaluation of snow sublimation rates (section 6.3) and the orographic dependence of precipitation based on empirical relationships (section 6.4) and on an atmospheric model (section 6.5). In section 7, simple hydrological budgets are computed in view of the former results. Finally, our conclusions are presented in section 8.

## 2. Climatic Conditions

[5] The climate of the Norte Chico region (Figure 1) varies from extremely arid in the north (26°S [e.g., Messerli *et al.*, 1996; Vuille and Amman, 1997; Kull *et al.*, 2002]) to Mediterranean in the south (33.5°S [e.g., Falvey and Garreaud, 2007]). The region is bounded by the Pacific Ocean and the high Andes, both of which have a strong impact on local climate. Westerly winds prevail above 4 km [Kalthoff *et al.*, 2002] while below this height winds tend to flow southward along the mountain range [Kalthoff *et al.*, 2002]. Along the coast an extensive deck of stratocumulus is often observed due to a very stable lower troposphere and relatively cold sea surface temperature (i.e., the Humboldt Current) [Garreaud *et al.*, 2002]. At low altitudes, sea breezes can carry air from the ocean, providing moisture for dew deposition, an important water supply for natural vegetation in coastal areas [Luebert and Plissock, 2006], especially during dry years [Kalthoff *et al.*, 2006; Khodayar *et al.*, 2007; Squeo *et al.*, 2007]. Inland, above the marine boundary layer, the air is extremely dry (relative humidity < 40% [Kull *et al.*, 2002]) and cloud free [Kull *et al.*, 2002]. As a consequence, shortwave radiation is particularly strong in the Andes.

[6] The annual precipitation has a pronounced orographic dependence, varying between 25 and 300 mm a<sup>-1</sup> from coastal areas to the cordillera (Figure 2a). A marked decline is also observed from the south to the north (Figure 2a [Luebert and Plissock, 2006]). The seasonal cycle of precipitation is very pronounced (Figure 2b), with most occurring in winter (between May and September; Figure 2b) during the passage of frontal systems from the Pacific [e.g., Escobar and Aceituno, 1998]. Small amounts of convective snowfall also occur at high elevations during summer [Begert, 1999; Kull *et al.*, 2002; Luebert and Plissock, 2006]. Summer precipitation is linked to a distinct, albeit episodic mode of climate variability characterized by periods of strong upper-level easterlies due to Rossby wave dispersion and modulation of the position of the Bolivian High [Vuille and Keimig, 2004]. Extended dry spells are not uncommon, and periods without precipitation may last 12 months. The interannual variability of precipitation is strongly linked to ENSO (El Niño Southern Oscillation), whose warm phase is generally associated with higher than usual precipitation [e.g., Aceituno, 1988; Rutllant and Fuenzalida, 1991; Escobar and Aceituno, 1998; Ginot *et al.*, 2006].

[7] Temperature also displays a strong seasonal cycle, which is linked to the annual cycle of radiation intensity [e.g., Kull *et al.*, 2002]. For instance, in Cerro Tapado glacier area, at 4215 m asl, mean temperature during 1998–1999 hydrologic year was  $-0.4^{\circ}\text{C}$ , with daily temperature ranging between  $-12$  and  $10^{\circ}\text{C}$  [Kull *et al.*, 2002]. The minimum occurs in June–August, coinciding with precipitation maximum (Figure 2b) and hence snowfall occurs over large areas (up to about 50% of total area; see section 6.2). Due to the time lag between snow accumulation and melt, maximum river discharge occurs about 4 months

**Table 1.** Rain Gauge Stations Used in This Study

ID Number	Watershed	Station	Altitude (m asl)	Precipitation (mm a <sup>-1</sup> )	Latitude	Longitude	Period
P1	COPIAPO	Jorquera En La Guardia	1800	50	27°45'S	69°40'W	1971–2005
P2	COPIAPO	Manflas Hacienda	1410	47	28°07'S	69°58'W	1971–2005
P3	COPIAPO	Lautaro Embalse	1110	41	27°59'S	70°00'W	1971–2005
P4	COPIAPO	Los Loros	940	37	27°50'S	70°07'W	1971–2005
P5	COPIAPO	Copiapo	385	19	27°21'S	70°21'W	1971–2005
P6	HUASCO	Conay	1450	90	28°58'S	70°09'W	1993–2005
P7	HUASCO	El Parral (Tambos before 1993)	1300	75 (78 before 1993)	28°59'S	70°12'W	1993–2005
P8	HUASCO	El Transito Reten (DMC)	1200	59	28°55'S	70°16'W	1993–2005
P9	HUASCO	El Transito	1100	56	28°52'S	70°17'W	1993–2005
P10	HUASCO	San Felix	1150	62	28°56'S	70°28'W	1993–2005
P11	HUASCO	Junta Del Carmen	770	50	28°45'S	70°29'W	1993–2005
P12	HUASCO	Santa Juana	560	44	28°40'S	70°39'W	1993–2005
P13	HUASCO	Vallenar (DGA)	420	41	28°35'S	70°44'W	1993–2005
P14	HUASCO	Freirian	100	38	28°30'S	71°05'W	1993–2005
P15	ELQUI	La Laguna	3100	161	30°12'S	70°02'W	1964–2005
P16	ELQUI	Juntas	2155	110	29°58'S	70°06'W	1990–2005
P17	ELQUI	La Ortiga	1560	158	30°12'S	70°29'W	1990–2005
P18	ELQUI	Cochiguaz	1560	112	30°08'S	70°24'W	1990–2005
P19	ELQUI	Los Nichos	1350	134	30°09'S	70°30'W	1990–2005
P20	ELQUI	Pisco Elqui	1300	105	30°07'S	70°30'W	1990–2005
P21	ELQUI	Huanta	1240	65	29°50'S	70°23'W	1990–2005
P22	ELQUI	Monte Grande	1155	86	30°05'S	70°30'W	1990–2005
P23	ELQUI	Rivadavia	850	104	29°58'S	70°34'W	1964–2005
P24	ELQUI	Vicuña (INIA)	730	105	30°02'S	70°42'W	1990–2005
P25	ELQUI	La Serena-La Florida (DMC)	142	90	29°54'S	71°12'W	1870–2005
P26	ELQUI	Almendral	430	94	29°59'S	70°54'W	1990–2005
P27	LIMARI	Pabellon	1920	149	30°24'S	70°33'W	1969–2005
P28	LIMARI	Las Ramadas	1350	308	31°01'S	70°35'W	1969–2005
P29	LIMARI	Tascadero	1230	272	31°01'S	70°40'W	1969–2005
P30	LIMARI	Hurtado	1200	138	30°17'S	70°41'W	1969–2005
P31	LIMARI	Tulahuen	1020	224	30°58'S	70°46'W	1969–2005
P32	LIMARI	Cogoti 18	905	182	31°05'S	70°57'W	1969–2005
P33	LIMARI	Combarbala	870	227	31°10'S	71°00'W	1977–2005
P34	LIMARI	Rapel	870	176	30°43'S	70°47'W	1969–2005
P35	LIMARI	Caren	740	188	30°51'S	70°46'W	1969–2005
P36	LIMARI	Pichasca	725	125	30°23'S	70°52'W	1969–2005
P37	LIMARI	Samo Alto	680	100	30°24'S	70°56'W	1969–1988
P38	LIMARI	Cogoti Embalse	650	174	31°00'S	71°05'W	1969–2005
P39	LIMARI	Placilla	600	232	30°53'S	71°19'W	1989–2005
P40	LIMARI	Tome	475	160	30°49'S	70°58'W	1969–2005
P41	LIMARI	Paloma Embalse	430	131	30°42'S	71°02'W	1969–2005
P42	LIMARI	Recoleta Embalse	400	101	30°30'S	71°06'W	1969–2005
P43	LIMARI	Pena Blanca	360	147	30°54'S	71°12'W	1989–1999
P44	LIMARI	Sataqui	280	120	30°37'S	71°07'W	1969–2005
P45	LIMARI	Punitaqui	280	162	30°49'S	71°15'W	1962–2005
P46	LIMARI	Ovalle	234	105	30°36'S	71°12'W	1969–2005
P47	LIMARI	La Torre	120	121	30°37'S	71°22'W	1969–2005
P48	CHOAPA	Las Burras	1250	231	31°34'S	70°49'W	1990–2005
P49	CHOAPA	Cuncumen	1080	285	31°56'S	70°37'W	1990–2006
P50	CHOAPA	San Agustin	1050	246	31°44'S	70°50'W	1990–2005
P51	CHOAPA	La Tranquilla	975	277	31°54'S	70°40'W	1990–2005
P52	CHOAPA	La Canela (DMC)	850	158	31°34'S	70°55'W	1990–2005
P53	CHOAPA	Coiron	840	298	31°54'S	70°46'W	1961–1989
P54	CHOAPA	Huintil	650	224	31°34'S	70°59'W	1990–2005
P55	CHOAPA	Salamanca	510	235	31°46'S	70°58'W	1990–2005
P56	CHOAPA	Mal Paso	375	237	31°45'S	71°06'W	1990–2005
P57	CHOAPA	Limahuida	295	183	31°45'S	71°10'W	1990–2005
P58	CHOAPA	Illapel	290	178	31°38'S	71°11'W	1990–2005
P59	CHOAPA	Puerto Oscuro	140	191	31°25'S	71°34'W	1911–2005

**Table 2.** Runoff Stations Used in This Study

ID number	Watershed	River	Station	Altitude (m asl)	Latitude	Longitude	Catchment Area (km <sup>2</sup> )	Period
R1	COPIAPO	Manflas	Vertedero	1550	28°09'S	69°59'W	1180	1968–2004
R2	COPIAPO	Pulido	Vertedero	1310	28°05'S	69°56'W	2108	1968–2004
R3	COPIAPO	Copiapo	Pastillo	1300	28°00'S	69°58'W	7467	1968–2004
R4	COPIAPO	Jorquera	Vertedero	1250	28°03'S	69°57'W	4150	1968–2004
R5	HUASCO	Transito	Angostura Pinte	1000	28°56'S	70°15'W	3220	1970–1989
R6	HUASCO	Carmen	San Felix	1150	28°56'S	70°28'W	2735	1970–1989
R7	HUASCO	Carmen	Ramadillas	825	28°45'S	70°29'W	2922	1970–1989
R8	HUASCO	Transito	Junta Rio Carmen	812	28°45'S	70°29'W	4153	1970–1989
R9	HUASCO	Huasco	Algodones	600	28°44'S	70°30'W	7187	1970–1989
R10	ELQUI	La Laguna	Embalse	3130	30°12'S	70°02'W	560	1966–2005
R11	ELQUI	El Toro	Junta La Laguna	2150	29°58'S	70°06'W	468	1990–1998
R12	ELQUI	Est. Derecho	Alcoguz	1645	30°13'S	70°30'W	345.1	1990–1998
R13	ELQUI	Cochiguaz	El Penon	1360	30°07'S	70°26'W	673.8	1990–1998
R14	ELQUI	Turbio	Varillar	860	29°57'S	70°32'W	4148	1918–2005
R15	ELQUI	Claro	Rivadavia	820	29°59'S	70°33'W	1502	1990–1998
R16	ELQUI	Elqui	Algarrobal	760	30°00'S	70°35'W	5729	1990–1998
R17	LIMARI	Hurtado	San Agustin	2035	30°28'S	70°32'W	656	1969–1988
R18	LIMARI	Combarbala	Ramadillas	1430	31°14'S	70°55'W	113	1969–1988
R19	LIMARI	Grande	Las Ramadas	1380	31°01'S	70°35'W	544	1969–1988
R20	LIMARI	Tascadero	Desembocadura	1370	31°01'S	70°40'W	238	1969–1988
R21	LIMARI	Cogoti	Fraguita	1065	31°07'S	70°53'W	475	1969–1988
R22	LIMARI	Grande	Cuyano	870	30°55'S	70°46'W	1262	1969–1988
R23	LIMARI	Pama	Valle Hermoso	850	31°16'S	70°59'W	154	1969–1988
R24	LIMARI	Mostazal	Caren	700	30°50'S	70°46'W	591	1969–1988
R25	LIMARI	Pama	Entrada Embalse Cogoti	680	31°05'S	71°04'W	700	1969–1988
R26	LIMARI	Cogoti	Entrada Embalse Cogoti	670	31°02'S	71°02'W	735	1969–1988
R27	LIMARI	Hurtado	Angostura De Pangue	500	30°26'S	71°00'W	1810	1969–1988
R28	LIMARI	Rapel	Junta	485	30°42'S	70°52'W	828	1969–1988
R29	LIMARI	Grande	Puntilla San Juan	420	30°42'S	70°55'W	3512	1969–1988
R30	LIMARI	Hurtado	Entrada Embalse	410	30°28'S	70°04'W	2228	1928–1988
R31	CHOAPA	Cuncumen	Bocatoma De Canales	1360	31°50'S	70°36'W	225	1974–1998
R32	CHOAPA	Choapa	Cuncumen	1200	31°58'S	70°35'W	1091	1918–2005
R33	CHOAPA	Illapel	Las Burras	1079	31°30'S	70°49'W	597	1990–1998
R34	CHOAPA	Chalinga	San Augustin	850	31°43'S	70°51'W	428	1974–1998
R35	CHOAPA	Chalinga	La Palmilla	800	31°42'S	70°43'W	242	1974–1998
R36	CHOAPA	Illapel	Huintil	775	31°34'S	70°58'W	928	1990–1998
R37	CHOAPA	Choapa	Salamanca	500	31°49'S	70°56'W	2253	1974–1998
R38	CHOAPA	Choapa	Limahuída	260	31°44'S	71°10'W	3644	1974–1998

later (October–December; Figure 2b). At low altitudes a two peak hydrograph is observed. First peak (in winter) is a response to liquid precipitation at low altitude whereas the second (spring/early summer) is related to snow and/or glacier melt.

### 3. Data and Methods

#### 3.1. Data

[8] The principal data upon which this study is based are precipitation from 59 rain gauges and runoff records from 38 river gauging stations of Norte Chico region (Tables 1 and 2; Figure 1). Data were provided by Chilean national water management institution (Dirección General de Aguas (DGA)) and meteorological institute (Dirección Meteorológica de Chile (DMC)). These stations are located in the watersheds of the Salado (northernmost), Copiapó, Huasco, Elqui, Limarí and Choapa (southernmost) rivers. The elevation of runoff gauging stations ranges between 260 m asl and 3130 m asl, and the area of the subcatchment under study ranges between 113 km<sup>2</sup> and 7467 km<sup>2</sup>. Data availability varies considerably between stations (Tables 1 and 2). The longest precipitation records are available from 1870 (La Serena, P25 in Table 1), and the longest discharge measure-

ments since 1918 (Choapa river at Cuncumen, R32 in Table 1). However, most of the study was performed with data recorded between 1968 and 2005.

[9] An important consideration is the possibility of biases in the discharge data due to irrigation in areas below 2000 m asl. If available (i.e., at 28 sites, 1950 onward), natural regime estimates were used [Alfaro and Honores, 2001; Ministerio de Obras Públicas–Dirección General de Aguas (MOP-DGA), 1984]. Natural regime estimates correspond to the discharge that would be observed if water extraction for irrigation and regulation by dams did not occur. They are computed from a statistical analysis of direct discharge measurements in the main irrigation canals that estimates the total water extraction over the whole irrigation network. The quality of the natural regimes estimates is not in the focus of the present study and the methodology is not fully described in this paper. However, this statistical analysis is subject to considerable uncertainty and both the direct discharge and natural regime estimates must be interpreted cautiously.

[10] Remotely sensed data were used to examine several aspects of the Norte Chico's cryosphere, including glacier and snow cover, focusing in particular on the high-altitude “La Laguna Embalse” catchment at the head of the Elqui Valley (Figure 1). First, a glaciological inventory of the

watershed upstream of the gauging station was made using both an ASTER (Advanced Spaceborne Thermal Emission and Reflection Radiometer) image and aerial photographs. The ASTER image was taken on 2 March 2003, has a spatial resolution of 15 m, and is numbered 25445. The aerial photographs (scale = 1/60,000) date from late summer 1978. Glacier delineation was manually performed on the 2003 ASTER image (visible spectral bands) without using any objective classification. Uncovered glaciers are easily recognizable in the satellite image. Rock glaciers were identified using the higher resolution aerial photography of 1978 and mapped onto the ASTER image. Geomorphologic criteria, such as steep lateral and frontal slopes and a surface structured by longitudinal and/or transverse ridges and furrows, were used to identify and delineate rock glaciers.

[11] Snow and ice indices were derived from MODIS (Moderate Resolution Infrared Spectrometer) images. The MOD10A2 snow cover data [Hall *et al.*, 2006] were used to assess snow duration. MOD10A2 is a binary estimate (snow/no snow) with a 500 m × 500 m spatial resolution. Data of snow distribution estimates are available each week, and a mosaic of 4 images was necessary to get information at the scale of the Norte Chico region. We studied monthly variation of the spatial extent from data registered between 26 February 2000 and 25 May 2003. The spatial extent of snow was then computed between 3000 and 4000 m asl, between 4000 and 5000 m asl and above 5000 m asl in the “La Laguna Embalse” catchment. The minimum altitude of snow cover was also computed for Elqui Valley.

[12] Finally, data from two atmospheric circulation models have been used. The first is the GFS (Global Forecast System) global atmospheric weather prediction model [Kanamitsu, 1989; Kalnay *et al.*, 1990] used to provide additional insight into the spatial and temporal variability of precipitation, especially its variation with altitude. The GFS model is a state-of-the-art numerical weather forecast system maintained by the United States National Center for Environmental Prediction (NCEP). The model represents the atmospheric state on a terrain following (sigma level) grid with an effective horizontal resolution of approximately 0.5° × 0.5°. It solves a hydrostatic version of the primitive equations and includes parameterization schemes for all important subgrid scale processes (radiation, clouds, gravity wave drag, boundary layer process, surface exchanges, etc.). Grid resolved precipitation (liquid and ice) is produced following Zhao and Carr [1997]. Convective precipitation is estimated using a modified Arakawa and Schubert [1974] parameterization scheme. GFS data from forecasts initialized twice daily (00:00 and 12:00 UTC) were available from late 2005 onward, so our analysis of GFS data will be largely restricted to the winter (May–September) of 2006. The data consist of two- and three-dimensional atmospheric fields at 6 hourly intervals. Those used in this study include the surface precipitation (grid scale and convective) rate, relative humidity and zonal wind. A time continuous data series was obtained by joining together hours 12 and 18 of each forecast. These forecast hours allow the model enough time to “spinup” precipitating weather systems, but are still sufficiently close to the initial time so that forecast error should have little impact on the results.

[13] The WRF (Weather Research and Forecasting) regional circulation model was used to assess sublimation in high-altitude areas. The WRF model is a modern, widely used atmospheric simulation code appropriate for spatial scales ranging from meters to thousands of kilometers. The model employs a nonhydrostatic dynamical core [Skamarock and Klemp, 2007] and with physical parameterization schemes for surface processes, planetary boundary layer (PBL), radiation and precipitation. Along with its atmospheric component, WRF permits the use of multilayer land surface models (LSM) to calculate surface heat fluxes and include simple treatment of snowpack development.

[14] Ten years (1970–1980) of hourly WRF output from a climate downscaling experiment with a spatial resolution of 15 km were available. The model was forced by the HADCM-3 “Baseline” climate scenario, which should be reasonably representative of the mean climatic conditions for the period 1960–1990 [Comisión Nacional de Medio Ambiente (CONAMA), 2007]. However, as the forcing data is not based on atmospheric analyses but global circulation model outputs, the model results cannot be expected to resemble the actual conditions during these years. The simulations made use of the Noah LSM [Chen and Dudhia, 2001] that includes a single layer snow component and simulates the snow accumulation, sublimation, melting, and heat exchange at snow-atmosphere and snow-soil interfaces. Other parameterization schemes employed include the PBL scheme of Hong and Pan [1996], the three-phase (snow included) microphysics of Hong *et al.* [1998], Kain-Fritsch convection [Kain and Fritsch, 1993], and shortwave and longwave radiation by Chou and Suarez [1994] and Mlawer *et al.* [1997], respectively.

[15] The WRF model is able to provide precipitation fields at 15 km resolution that could be used in hydrological analyses in the same way as for the GFS model. However, we find that the model drastically overestimates precipitation at high altitudes in central and northern Chile. For example, in the Elqui valley region WRF produces some 2500 mm a<sup>-1</sup> of precipitation, around 10 times the observed value. The same problem has been noted in other studies and with other mesoscale atmospheric models and with different boundary conditions [Rojas, 2006; Falvey and Garreaud, 2007], and its cause has yet to be explained. As a consequence of the over prediction of precipitation most regions above 3000 m asl show year-round snow cover, since snow accumulation during winter is so great that it is unable to completely melt or evaporate during the ablation season. Despite WRF’s over prediction of precipitation, we assume that the models descriptions of boundary layer processes and surface turbulent heat fluxes are sound, and able to produce reasonable estimates of sublimation over the Andean snowpack.

### 3.2. Methods

[16] For catchments including uncovered glaciers, rock glaciers (including debris covered glaciers) and nonglaciated areas, the hydrological balance can be expressed by

$$Q = (-B_g - E_g + P_g) \cdot S_g - B_{rg} \cdot S_{rg} + P_{ng} \cdot (S - S_g) - E_{ng} \cdot (S - S_g) - G + \varepsilon \text{ [m}^3\text{a}^{-1}\text{]} \quad (1)$$

[17] Where  $Q$  is the annual discharge measured at the outlet of the watershed,  $B_g$  is the specific mass balance of glaciers (expressed in  $\text{m a}^{-1}$ ),  $B_{rg}$  is the specific mass balance of rock and debris covered glaciers,  $P_g$  and  $P_{ng}$  refer precipitation over glacierized areas and over non-glacierized areas (including debris covered and rock glaciers),  $E_g$  and  $E_{ng}$  are mean annual evaporation (including transpiration and sublimation),  $S$ ,  $S_g$  and  $S_{rg}$  are respectively the surface of the watershed, of uncovered glaciers and of rock glaciers (including debris covered glaciers),  $G$  is mean groundwater flow and  $\varepsilon$  includes possible other terms of the water budget (for instance, the water budget of semipermanent snow, which remains longer than an annual cycle). As a sign convention, we assume that  $E_g$  and  $E_{ng}$  are positive (negative) when sublimation/evaporation (condensation) occurs.

[18] Considering the mean precipitation ( $P$ ) over the watershed, equation (1) can be written as follows

$$\frac{Q}{S} - P = D$$

$$= \frac{S_g \cdot (-B_g - E_g) - S_{rg} \cdot B_{rg} - E_{ng} \cdot (S - S_g) - G + \varepsilon}{S} [\text{mm a}^{-1}]$$

[19] Where  $D$  is the runoff deficit [e.g., Pouyaud *et al.*, 2005]. Generally,  $D$  is negative, indicating that part of the precipitation does not enter into surface streams. Conversely, a positive  $D$  value indicates water contributions from sources other than precipitation, such as glacial meltwater. Positive  $D$  values are likely to occur in watersheds with low water losses due to groundwater flow and sublimation/evaporation.

#### 4. Long-Term Precipitation and Discharge Variability

[20] In order to study the variability of precipitation and discharge over the 20th century, we examine historical annual precipitation records available at the coastal stations of La Serena (P25 in Table 1, 1870–2005) and Puerto Oscuro (P59, 1911–2005) and annual discharges (direct measurements, not natural regime estimates) on the Choapa (Cuncumen station, R32, 1918–2005) and Turbio (Varillar station, R14, 1918–2005) rivers.

[21] As already provided by Vuille and Milana [2007], the records at La Serena and Puerto Oscuro (Figure 3a) demonstrate that over the 20th century, precipitation in the Norte Chico has declined considerably [Santibañez, 1997; Le Quesne *et al.*, 2006]. However, this decrease mainly occurred during the first 30 years of the century. At La Serena, between 1870 and 1908, relatively wet conditions (mean annual rainfall is  $162 \text{ mm a}^{-1}$  during this period) prevailed and droughts were largely absent. For instance, annual rainfall of less than  $30 \text{ mm a}^{-1}$  were only observed once in 39 years between 1870 and 1908, whereas such precipitation amounts were observed 10 times within 74 years between 1932 and 2005 (that is 5 times more often). An abrupt change occurred around 1908, when mean precipitation over the following decade decreased by 50% (Figure 3b). The mean annual precipitation increased between 1920 and 1930, but dropped again around 1932. From this time onward, lower precipitation (mean annual precipitation is  $93 \text{ mm a}^{-1}$  over the period 1932–2005) has been consistently observed [CONAMA, 2007]. Additional

evidence of relatively stable precipitation throughout most of the 20th century has been provided by analysis of the Cerro Tapado deep ice core [Ginot *et al.*, 2006], which does not reveal any significant change in accumulation since 1920. The most significant droughts were observed around 1910 and 1970, whereas the heaviest precipitation years after 1926 were 1987 and 1997, both associated with El Niño events.

[22] The discharge measurements of Choapa and Turbio rivers show similar patterns of long term variability. Indeed, the annual precipitation and discharge are significantly correlated during the 20th century (correlation between Choapa discharge at Cuncumen and precipitation at Puerto Oscuro is  $R = 0.87$ ,  $n = 76$ ,  $p = 0.0005$ ). We are aware that discharge must be interpreted with caution due to water recollection for irrigation, but discharge was clearly higher before 1930 than after 1930. Notably, in the later part of this century (1966 onward) a weak increasing trend is observed (solid lines), as also noted by Novoa *et al.* [1995, 1996] and Novoa [2006], which may be related to slight increase in precipitation during the same period (Figure 3c, dashed lines). However, these increasing trends have very low statistical significance and are not conclusive.

[23] Although reliable long term measurements of discharge at higher altitudes are scarce in the Norte Chico region, 40 years of discharge (1966–2005) and precipitation (1964–2005) are available at La Laguna Embalse station (R10, P15 in Tables 1 and 2), situated in the La Laguna River watershed at 3130 m asl. The annual series at La Laguna are not 100% complete, and occasional data gaps were filled using linear regression with discharge of Turbio river (at Varillar, R14) and precipitation measurements at Rivadavia station (P23, 850 m asl, close to Turbio river at Varillar). Discharge values are significantly correlated between the two sites ( $R = 0.93$ ,  $n = 36$ ,  $p = 0.0005$ ), whereas precipitation presented weaker correlation ( $R = 0.76$ ,  $n = 41$ ,  $p = 0.0005$ ).

[24] Figure 4a displays the variation of precipitation and discharge at La Laguna Embalse. Even though the discharge increased from 1964 to 1990 as suggested by Novoa *et al.* [1995, 1996] and Novoa [2006], it is associated with a corresponding increase in precipitation, suggesting that variations of discharge and precipitation amounts are closely related. Moreover, no significant trend is observed over 1964–2005, neither for precipitation nor discharge. Hence any increase in glacial melt in the La Laguna watershed over the last 50 years (if this even occurred) was apparently not sufficient to produce a significant increase in discharge. This point will be discussed further in section 6.

#### 5. Precipitation and Discharge in High-Elevation Areas

[25] The runoff coefficient and runoff deficit [e.g., Pouyaud *et al.*, 2005] were computed for all catchments above 250 m asl (Table 1), using discharge and precipitation data over similar periods for subcatchments and for the main catchment (Table 2). Although natural regimes were used to compute runoff coefficients, data from catchments located below 1000 m asl must be considered with caution. Over large watersheds, precipitation is only available for subcatchments. In order to distribute precipitation over the whole catchment, a basic interpolation was applied. We

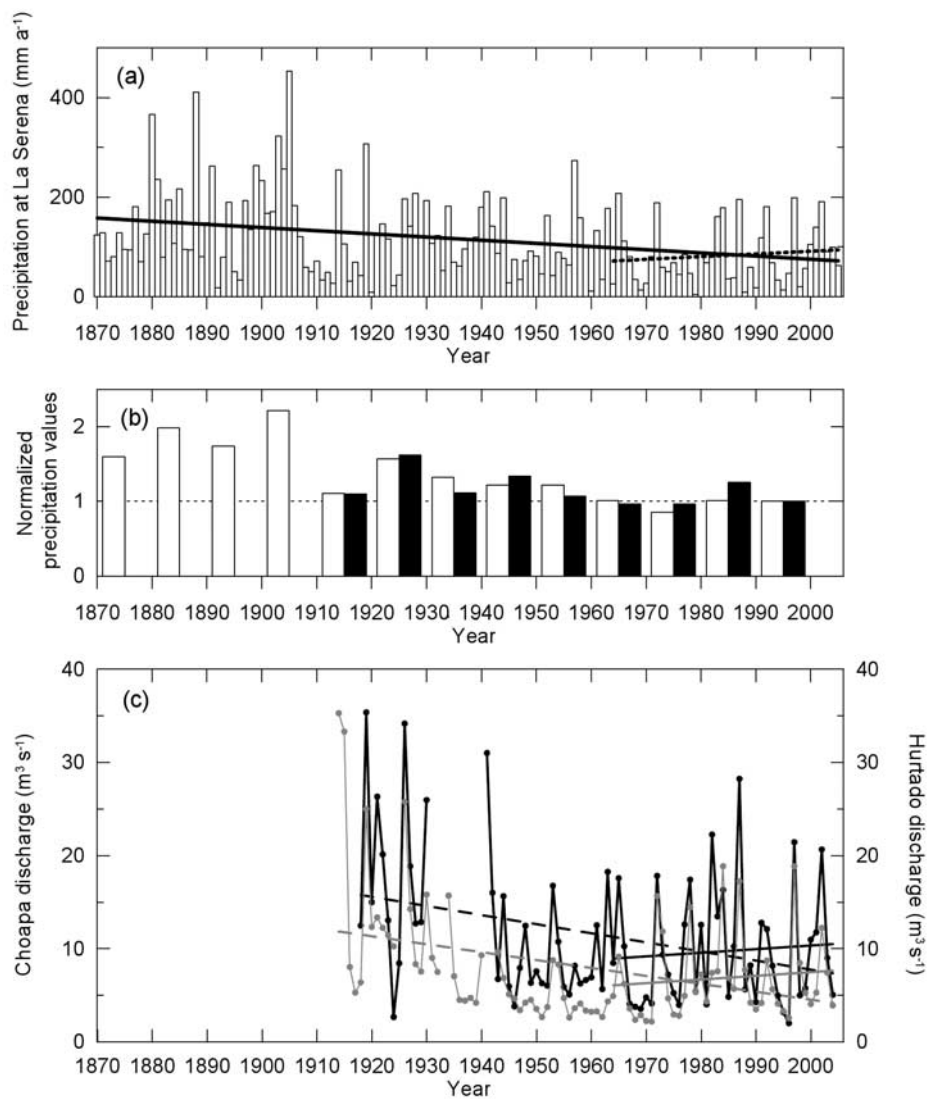


**Figure 3.** Historical variation of precipitation and discharge. (a) Annual precipitation at La Serena (P25 in Figure 1, 142 m asl) between 1870 and 2005. Continuous and dashed lines are linear regressions for the periods 1870–2005 and 1964–2005, respectively. Precipitation decrease at La Serena between 1870 and 2005 is significant ( $p = 0.001$ ), whereas no significant trend was observed after 1964. (b) Normalized decadal precipitation at La Serena (open bars) and Puerto Oscuro (black bars, P59 in Figure 1). Data are normalized by dividing decadal precipitation by the mean precipitation during the decade 1991–2000. (c) Annual discharge between 1918 and 2005. Dotted black line is discharge of Choapa River at Cuncumen data (R32 in Figure 1, 1200 m asl), and dotted gray line is discharge of Turbio River at Varillar (R14 in Figure 1, 860 m asl). Continuous and dashed lines are linear regressions for the periods 1918–2005 and 1950–2005, respectively. The runoff decrease of Turbio River and Choapa River between 1918 and 2005 is significant ( $p = 0.006$ ), whereas the observed increase after 1950 is not statistically significant.

consider two catchments  $S_1$  and  $S_2$  (Figure 5), whose areas are defined by outlet points  $R_1$  and  $R_2$  (runoff gauging stations). The catchment  $S_1$  is included in  $S_2$ . The rain gauge  $P_1$  is located within  $S_1$  whereas  $P_2$  and  $P_2'$  are located in  $S_2$  but not in  $S_1$ . Precipitation  $P_1$  is considered as representative over  $S_1$ . Over  $S_2$  the precipitation value corresponds to the mean of  $P_2$  and  $P_2'$  (or is  $P_2$  if only one rain gauge is located in this area), except in the part occupied by  $S_1$  where precipitation is  $P_1$ . This method was applied to each catchment and subcatchment.

[26] Runoff coefficients increase strongly with altitude (Figure 6), and actually exceed 100% in several of the

highest catchments. Moreover, runoff deficit values are more negative at low elevation than at high elevation. Runoff coefficients are especially large in high-altitude catchments of the Elqui, Limarí and Choapa valleys, where maximum values are 130%, 180% and 193%, respectively, with associated runoff deficits of 31 mm w.e.  $a^{-1}$ , 182 mm w.e.  $a^{-1}$  and 232 mm w.e.  $a^{-1}$ , respectively. In the La Laguna watershed, runoff deficit is low ( $-27$  mm w.e.  $a^{-1}$ ) indicating that discharge is roughly equal to the net precipitation input. The very high runoff values suggest that water losses (groundwater flow and sublimation/evaporation) are likely to be low in the area, and/or that gains (precipitation

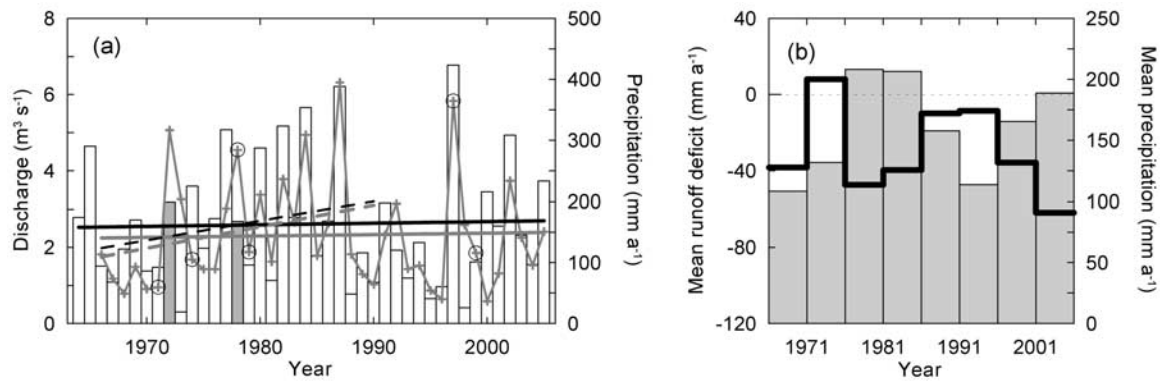


**Figure 4.** Historical variation of precipitation and discharge at the high-elevation La Laguna Embalse station (P15 and R10 in Figure 1,  $30^{\circ}12'S$ ,  $70^{\circ}03'W$ , 3130 m asl). (a) Open bars are annual precipitation, and solid gray lines are annual discharge. Missing precipitation and discharge data that were replaced by measurements downstream at the Varillar station (P23 and R14 in Figure 1,  $29^{\circ}56'S$ ,  $70^{\circ}32'W$ , 860 m asl) are indicated by gray bars and open circles, respectively. Continuous and dashed black lines are precipitation trends over the periods 1964–2005 and 1966–1990, respectively. Continuous and dashed gray lines are discharge trends over the periods 1964–2005 and 1966–1990, respectively. Continuous and dashed gray lines are discharge trends over the periods 1964–2005 and 1966–1990, respectively. Runoff and precipitation increasing trends over the period 1964–1990 only have a low level of significance ( $p = 0.06$ ), and no significant trend is observed for the period 1964–2005. (b) Variation of 5-year mean precipitation and runoff deficit at La Laguna Embalse station between 1966 and 2005. Gray columns are mean precipitation, and black line is mean runoff deficit.

or water contribution from cryosphere) are underestimated. These possibilities are examined hereafter in sections 6 and 7.

## 6. Characterization of High-Altitude Watersheds

[27] In this section we examine several characteristics of the high-altitude catchments of the Norte Chico, where discrepancies between precipitation and runoff are particularly large. Our principal (but not unique) objective is to derive broad but realistic estimates of the contribution to the hydrological balance from processes of glacial retreat, snow sublimation and orographic precipitation. In all cases we make use of observational data, and complement these where appropriate with the results of atmospheric models.

### 6.1. Glacier Extent and Retreat

[28] The spatial extent of the cryosphere (glaciers) in the Norte Chico region has not been comprehensively estimated in the past [Garin, 1987; Rivera *et al.* 2000, 2002; Brenning, 2005]. Most studies have focused on climatic conditions during the late Pleistocene obtained from the interpretation of moraine positions [Kull *et al.*, 2002; Zech *et al.*, 2006], or on climatic variations during the 20th century derived from a deep ice core drilled down to the bedrock at Cerro Tapado summit (at 5536 m asl,  $30^{\circ}08'S$ ,  $69^{\circ}55'W$ ; Figure 1 [e.g., Stiehler *et al.*, 2001; Ginot *et al.*, 2001, 2006]), an isolated ice mass at 5500 m altitude, surrounded by almost ice-free mountains as high as 6000 m [Kull *et al.*, 2002].

[29] Here we estimate the runoff contribution from glaciers to the discharge in the La Laguna Embalse catchment, one of the most glacierized basin in the area and containing the Cerro Tapado glacier. In order to estimate water production from the cryosphere, we performed a glacier inventory (see section 3.1 for method). We estimated that 34 (uncovered) glaciers have a total surface area of about  $4.4 \text{ km}^2$ . Moreover, 46 rock and debris covered glaciers were found and represent additional  $10.6 \text{ km}^2$ . This amounts

to 1% and 2% of the total surface area ( $560 \text{ km}^2$ ) of the catchment.

[30] In order to determine the water contribution due to the retreat of these glaciers we use mass loss estimates available in the literature. Rivera *et al.* [2002] used observations of the Tronquitos glacier ( $28^{\circ}32'S$ ,  $69^{\circ}43'W$ ; Figure 1) between 1955 and 1984 to make a rough estimate of the mass loss from high-altitude glaciers between 1945 and 1996 in the Norte Chico region (although no comparison was made with local discharge). They estimated the volume of ice from areas where glaciers totally vanished (the 11.4% of glacier areas) assuming that ice thickness in these areas ranged between 30 and 50 m before melting. Moreover, to assess melting discharge from ice covered surfaces (the 88.6% remaining), they assumed that mean AAR (Accumulation Area Ratio, i.e., ratio of the glacier's accumulation area to the glacier's total area) of the glaciers was 56% and that glacier thickness experienced no change in its accumulation area and decreased with a mean rate of 0.7 to 1.4 m

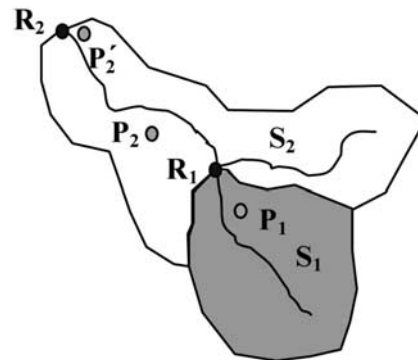


**Figure 5.** Example of the methodology used to estimate catchment scale precipitation for runoff coefficient calculations.

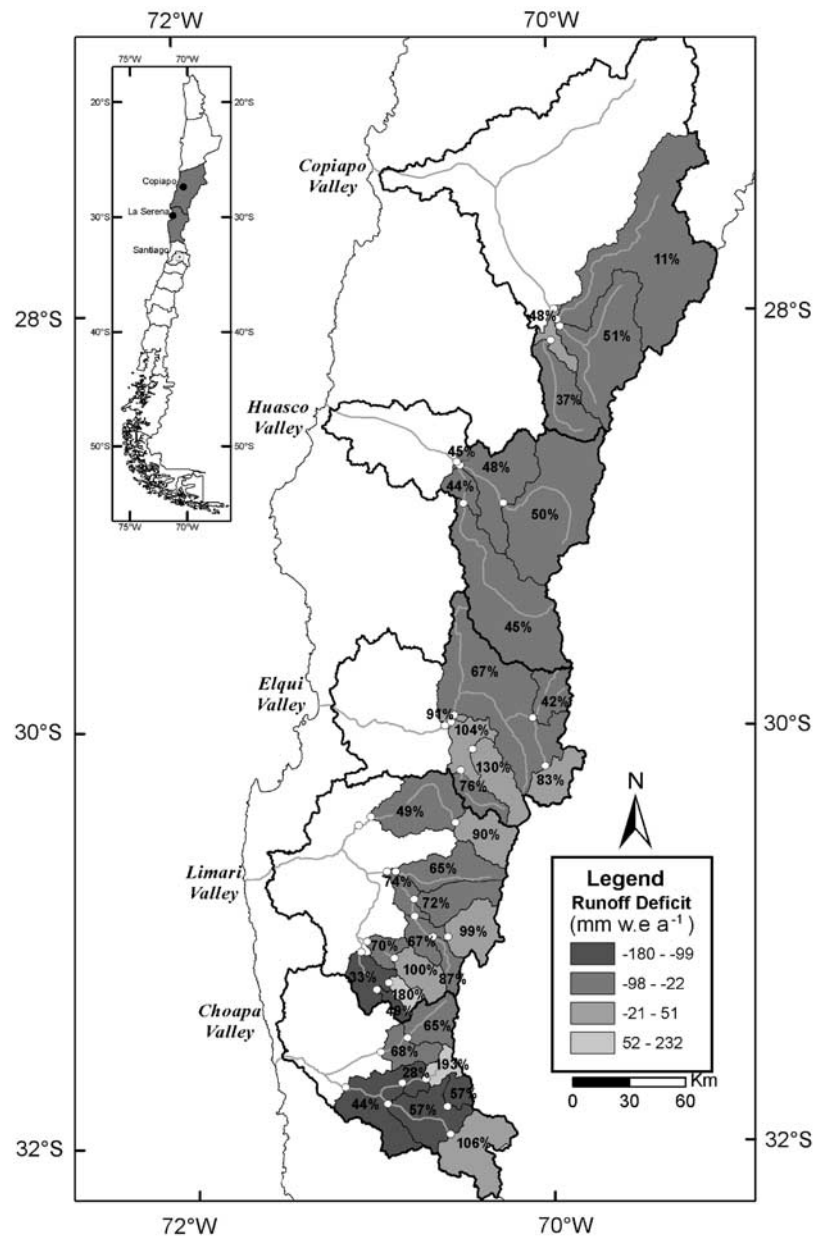


**Figure 6.** Runoff coefficients and runoff deficit values (in mm w.e. a<sup>-1</sup>) for catchments in the Norte Chico region.

a<sup>-1</sup> in the ablation area. Although the concept of AAR should be cautiously considered in the area (Rabatel et al., Cold glaciers behavior in the semiarid Andes of Chile (29°S): Results of a 6-year monitoring program, submitted to *Journal of Glaciology*, 2008, hereinafter referred to as Rabatel et al., submitted manuscript, 2008), this leads to a mean specific mass balance between -0.3 and -0.6 m w.e. a<sup>-1</sup>. This value is very similar to the mean mass balance values of -0.15 m w.e. a<sup>-1</sup> and -1.0 m w.e. a<sup>-1</sup> that were measured on 6 glaciers in the nearby Pascua Lama area (29°20'S, 70°00'W; Figure 1) during 2002–2006 period (Rabatel et al., submitted manuscript, 2008).

[31] The *Rivera et al.* [2002] estimation was applied in order to assess the possible contribution of glacier retreat to discharge at the outlet of La Laguna Embalse, using the glacier inventory data described previously. We assumed

that specific discharge from rock glaciers is about 2 to 3 times lower than from uncovered ice areas as suggested by *Krainer and Mostler* [2002] comparisons performed in the Alps. We also considered that ice loss was directly related to ice melt and not to sublimation. The estimated mean annual contribution from debris covered, rock and uncovered glaciers ranges between 110 and 200 L s<sup>-1</sup>. This value represents between 4% and 9% of the mean discharge at La Laguna Embalse runoff station between 1964 and 2005.

[32] Although the water contribution from glacial retreat is significant, it does not seem to have increased significantly over the last 50 years, as it has been suggested by some authors [CONAMA, 1999]. At least, if they occurred, glacier melt discharge variations were not sufficient to produce a significant increase in discharge (section 4). The behavior of Tronquitos glacier described by *Rivera et*

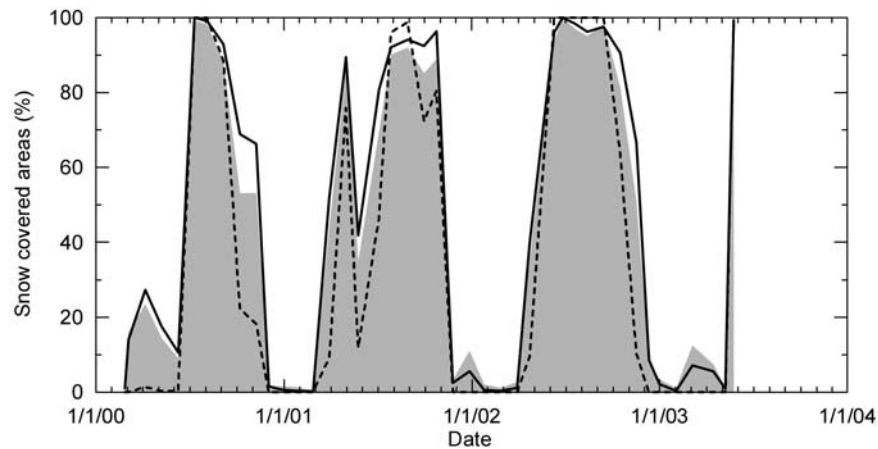


**Figure 7.** Snow cover extent over the La Laguna watershed, estimated from MOD10A2 snow cover indices between 26 February 2000 and 25 May 2003. The continuous line is snow extent as percentage of the total area between 4000 and 5000 m asl. The dashed line is snow extent between 3000 and 4000 m asl. The gray area represents snow extent over the entire watershed.

*al.* [2002] also suggests that melting discharge has not increased significantly since 1955. While the Tronquitos glacier experienced a faster retreat of its snout after 1984 ( $-14 \text{ m a}^{-1}$  and  $-23 \text{ m a}^{-1}$  between 1955–1984 and 1984–1996, respectively), melting occurred over a more reduced area. Hence assuming this faster retreat, we estimated that glacier melt contribution to discharge at La Laguna Embalse changed only within 15–20% between the two periods. This phenomenon has also been described by other authors. For instance, while glacier melt is currently enhanced in the Cordillera Blanca of Peru [e.g., *Mark and Seltzer*, 2003; *Mark and McKenzie*, 2007], *Pouyaud et al.* [2005] suggest that melting discharge will increase only during the next 25–50 years but will next decrease due to the reduction of glacier surfaces. Melting increase should therefore have been too small to be clearly observed at La Laguna Embalse runoff station.

## 6.2. Snow Cover

[33] The relatively limited glacial coverage in the Norte Chico indicates that snow will make the largest contribution in discharge in high-altitude catchments. To verify this point, we studied variation of the spatial extent of snow cover with the MOD10A2 snow cover data from February 26, 2000 to May 25, 2003 in order to assess snow duration. 42 mosaics of 4 images were processed, giving monthly extent of snow over the Norte Chico region. Results are presented in Figure 7. Snow covers 80% of La Laguna Embalse catchment during 4 months on average (12 months over the 3 years of study) with a minimum of 2.5 months in 2000 and a maximum of 5 months in 2002. Snow extent exceeds 50% during about 6 months on average. The minimum altitude with snow is generally about 1200 m asl. Maximum snow extent generally occurs in June–August, after strong snow precipitation events. It decreases rapidly from October onward, due to the lack of precipitation. Snow accumulation and depletion occur very rapidly, over periods of about 1 or 2 months and more or less simultaneously over the entire catchment (snow duration at 3000 m asl is only one month shorter than at 5000 m asl). Frequent but not intense precipitation in the area may

explain this behavior. Indeed, even at low elevations ( $\sim 3000 \text{ m asl}$ ), snow precipitation generally occurs at least one to two times each month in winter. In such conditions, winter ablation above 3000 m asl is continuously compensated by fresh snow. However, except in particularly strong accumulation points such as cornices (where glaciers are formed), accumulation is always very low and snow disappears quickly if not renewed frequently. Hence snow disappears quickly everywhere over the catchment 1 or 2 months after the last precipitation event of winter.

[34] Combined with short-term glacier mass balance variations, snow fall may also play an important role in the long-term variation of discharge. Figure 4b shows the mean 5-year precipitation and runoff deficit, calculated assuming that the precipitation recorded at the La Laguna site is representative of the precipitation in the entire catchment. The runoff deficit (Figure 4b) at La Laguna Embalse station is strongly negative during important precipitation periods (1976–1985 and 1996–2005), suggesting that part of the net precipitation does not contribute to discharge. This may be due to storage by snowpack or by permafrost after refreezing of melted snow within the active layer. Conversely, during periods of relatively low precipitation (1966–1976 and 1986–1996), the runoff deficit is close to zero or even positive. These values suggest that discharge is larger than available water by precipitation, suggesting a significant contribution by melting of snow and ice.

## 6.3. Sublimation at High Altitudes

[35] In high-altitude areas of Norte Chico region very little sublimation data are available. Summer sublimation has been assessed from direct lysimeter measurements performed by *Stichler et al.* [2001] on Cerro Tapado Glacier between 11 February and 16 February 1999 (summertime) yielded sublimation rates of  $2\text{--}4 \text{ mm w.e. day}^{-1}$ . Direct measurements of summer sublimation performed in Pascua Lama glacierized area between December 2007 and March 2008 suggest slightly lower mean values between  $1.26 \text{ mm w.e. day}^{-1}$  and  $2.25 \text{ mm w.e. day}^{-1}$  (*Castebrunet et al.*, Surface energy balance on subtropical glaciers of high

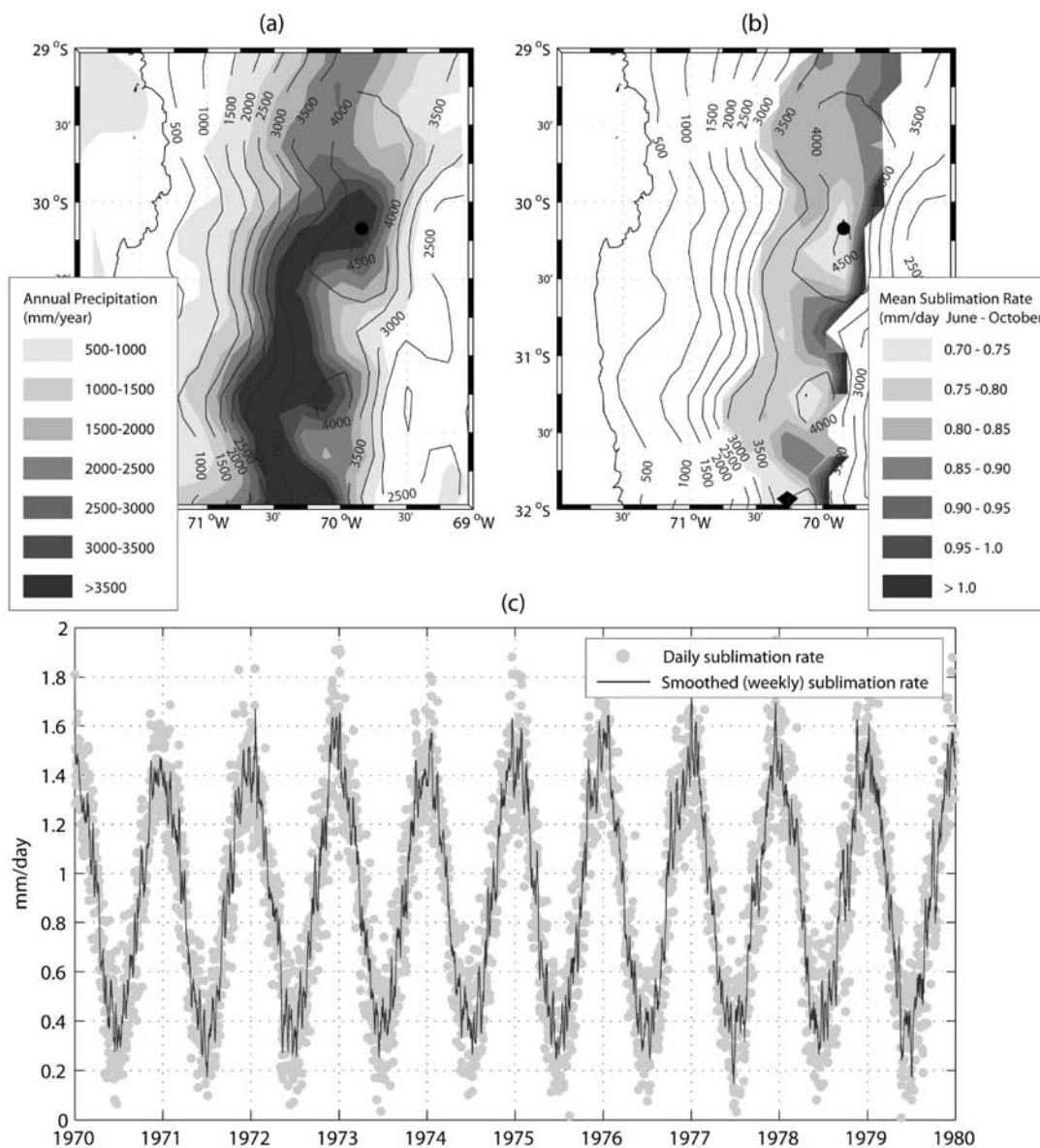


**Figure 8.** (a) Annual mean precipitation (rain + snow) simulated by WRF for the period 1970–1980. Black contour lines represent the model topography and coastline. (b) Mean daily sublimation rate during winter and spring (June–October, inclusive) at model grid points where snow is present at least 90% of the time. (c) Time series of daily sublimation rates (gray circles) at the point indicated by the black circle in Figures 8a and 8b. The solid line shows the sublimation after applying a 7-day smoothing filter.

altitude (5,000 m asl) in the semiarid Andes of Chile (29°S), submitted to *Geophysical Research Letters*, 2008, herein-after referred to as Castebrunet et al., submitted manuscript, 2008). However, sublimation rate is likely to be lower in winter. The best source of information was obtained on Cerro Tapado glacier, where, from the interpretation of chemical enrichment of ice (post deposit processes), *Ginot et al.* [2006] estimated a mean annual sublimation of 327 mm w.e.  $a^{-1}$  for 1962–1999 period. This value is close to other annual mean estimations obtained at similar altitudes at tropical latitudes in Ecuador or Bolivia [*Favier et al.*, 2004; *Wagnon et al.*, 1999]. Assuming that sublimation acts continuously at a constant rate during the 4 months when snow cover is present (section 6.2) over more than 80% of catchment area, water loss from winter sublimation should be 87 mm w.e.  $a^{-1}$ .

[36] The WRF model simulations provide additional information on sublimation. We studied the model data from a point located near the Elqui valley at 4000 m asl. (Figure 8). In the model, precipitation is substantially overestimated (Figure 8a), since modeled snow accumulation exceeds 2500 mm w.e.  $a^{-1}$  (in the region, we expect precipitation somewhere between 200 and 500 mm  $a^{-1}$ ) and does not entirely melt in summer. However, sublimation results may still be representative of the values observed over a permanent snow surface or over glaciers (without penitents). The year-round presence of a snowpack allows examination of complete annual cycles of sublimation for snow/ice areas. The annual mean sublimation rate is equivalent to a net annual water loss of  $\sim 365$  mm  $a^{-1}$ , which is very close to *Ginot et al.* [2006] estimates for Cerro Tapado glacier. The sublimation series show a relatively stable

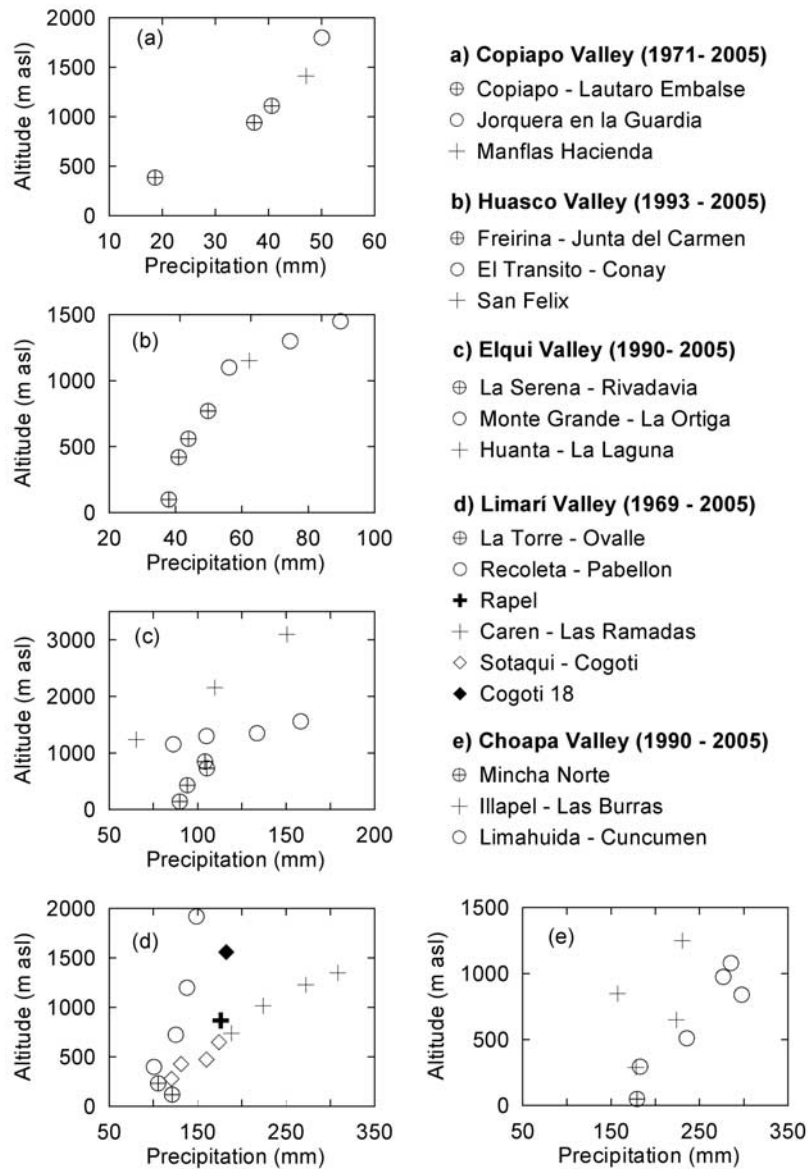


**Figure 9.** Variation of the mean annual precipitation with elevation in Choapa (South), Limari, Elqui, Huasco, and Copiapo (North) valleys.

seasonal variation between  $\sim 0.4 \text{ mm day}^{-1}$  in winter and  $\sim 1.5 \text{ mm day}^{-1}$  in summer (Figure 8c). Mean values in summer are only slightly less than measurements performed by *Stichler et al.* [2001] but are of the same order than measurements performed by Castebrunet et al. (submitted manuscript, 2008). This suggests a good representativeness of WRF sublimation, which should also be observed in winter. Considering that sublimation of snow is (in reality) only effective during  $\sim 4$  months in winter leads to a mean sublimation of about  $80 \text{ mm w.e. a}^{-1}$  where snow is observed. This situation is only observed over 80% of the catchment area and the net annual mean distributed sublimation of snow areas should be about  $64 \text{ mm w.e. a}^{-1}$ . Examination of model results at other locations indicates that sublimation rates over snow are quite uniform over the Norte Chico region, irrespective of the topographic elevation and latitude (Figure 8b).

[37] Measurements performed at Ilimani summit ( $16^\circ\text{S}$ , Bolivian Andes) during wintertime [*Wagnon et al.*, 2003], and at Antarctica [*Bintanja and Van den Broeke*, 1995] partly give justification to the assumption of significantly lower sublimation rates during winter. On cold glaciers or cold snow surfaces, due to the absence of melting, the energy available as net radiation is used to increase surface temperature and the turbulence of the surface boundary layer and is hence converted in turbulent fluxes [*Wagnon et al.*, 2003]. The higher the net radiation, the stronger the turbulent heat fluxes. For instance, *Wagnon et al.* [2003, Figure 13] represent turbulent heat flux versus net radiation, and this clearly shows a linear relationship between these two variables in the case of cold glacier. In winter, the high albedo of fresh snow and weak incoming longwave radiation due to the cold and thin atmosphere in high-altitude areas may therefore induce low net radiation values that may justify low sublimation. Measurements under con-

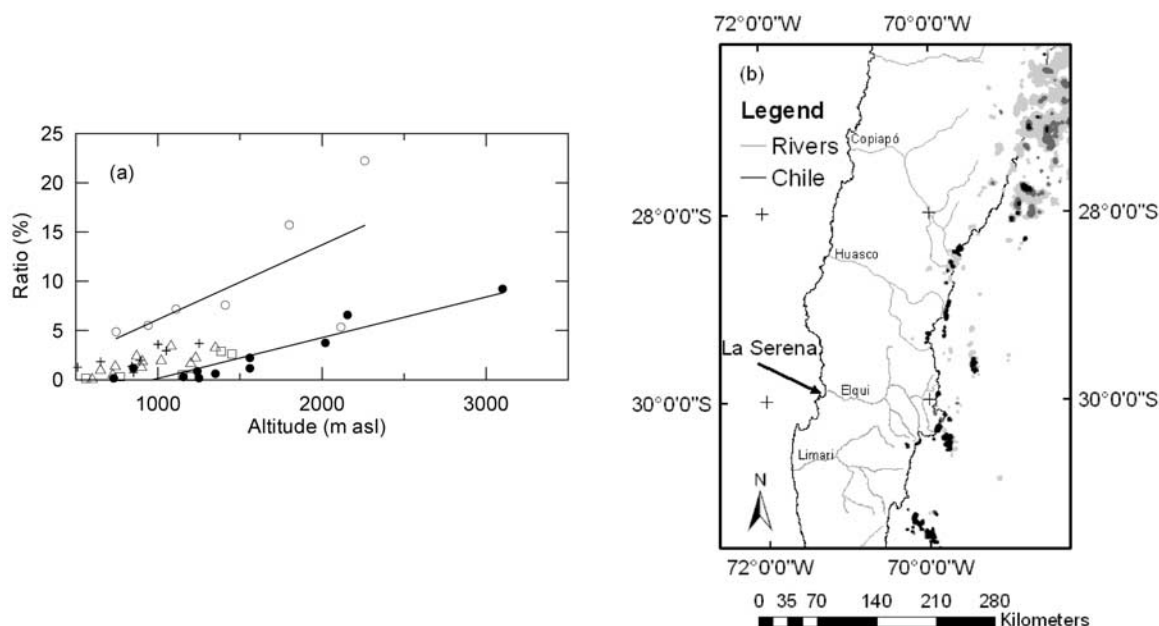


**Figure 10.** (a) The contribution of summer precipitation (December–March) to the mean annual precipitation (1993–2005). Crosses are data in Choapa valley, triangles are data in Limari valley, dots are data in Elqui valley, squares are data in Huasco valley, and open circles are data in Copiapo valley. (b) Examples of summertime snow extent over Norte Chico region obtained from MOD10A2 snow cover data. Black, dark gray, and bright gray points are snow-covered areas on 26 December 2000, 25 January 2001, and 26 February 2001, respectively.

trolled conditions in laboratory also suggest that at very low temperature (at  $-35^{\circ}\text{C}$ ) the low saturated vapor pressure impedes sublimation because the air near the ice surface is saturated with water vapor [Bergeron *et al.*, 2006]. Finally, high sublimation values in semiarid Andes are generally associated to snow penitents usually observed in this area [e.g., Lliboutry, 1954; Corripio and Purves, 2005]. Penitent initiation and coarsening requires sublimation rather than melting [Bergeron *et al.*, 2006]. Nevertheless, while snow penitents are frequent in summer, they are almost absent until October–November suggesting that initiation phase of penitents is weak in winter.

#### 6.4. Observation of the Orographic Effect on Precipitation Using Field Data

[38] The spatial variation of annual precipitation is now examined using station data in the Choapa (9 stations), Limari (16 stations), Elqui (12 stations), Huasco (8 stations) and Copiapó (5 stations) river valleys (Table 1). The mean annual totals were computed over periods without data gaps. This was possible from 1990–2005 in the Choapa and Elqui valleys, 1969–2005 in the Limari valley, 1993–2005 in the Huasco valley and 1971–2005 in the Copiapo valley.

[39] The variation of mean annual precipitation with station altitude is shown separately for each valley in Figures 9a–9e. The altitude dependence is extremely strong. When examining each subvalley separately, nearly linear trends are observed with altitude, leading generally to precipitation around 2 to 3 times stronger at 3000 m asl than in coastal areas. The strength of the precipitation gradient appears to depend on the orientation of each subvalley. The orographic dependence is clearer in the northern part of the

study area than in the southern part where data scatter is more important (Figure 9a), but this may be because fewer observations are available in the northernmost valleys. Due to the lack of data in high-altitude areas, precipitation amounts cannot be assessed above 3100 m asl.

[40] The high runoff coefficients observed in the high-altitude catchments of the Norte Chico region suggest that the net orographic enhancement of precipitation may continue to higher altitudes where precipitation is not sampled. For example, Ginot *et al.* [2006] estimated that the mean annual snow accumulation on Cerro Tapado (5536 m asl) glacier between 1962 and 1999 was  $539 \text{ mm w.e. a}^{-1}$ . This is more than 3 times stronger than precipitation at La Laguna Embalse station (3100 m asl). Of course, snow accumulation on glaciers is expected to be higher than the mean regional precipitation to allow formation of glaciers in the area.

[41] Summer precipitation is only significant in high-altitude areas (Figure 10a), and is greatest in the northern part of the study area, where it represents about 25% of total precipitation at 2000 m asl, compared to less than 5% in the southern part. At high altitude summer precipitation occurs as snow, which is an important point for glacier response to climatic forcing. Examples of summertime snow cover obtained from MODIS data are shown in Figure 10b, where snow extent is progressively growing in the northern part of the study area from 26 December 2000 to 26 February 2001. These examples also indicate that summer snowfall is most dominant in the northern part of the study area.

#### 6.5. Insights From Atmospheric Model Data

[42] The lack of high-altitude precipitation data in the Norte Chico region leads us to seek alternative methods for

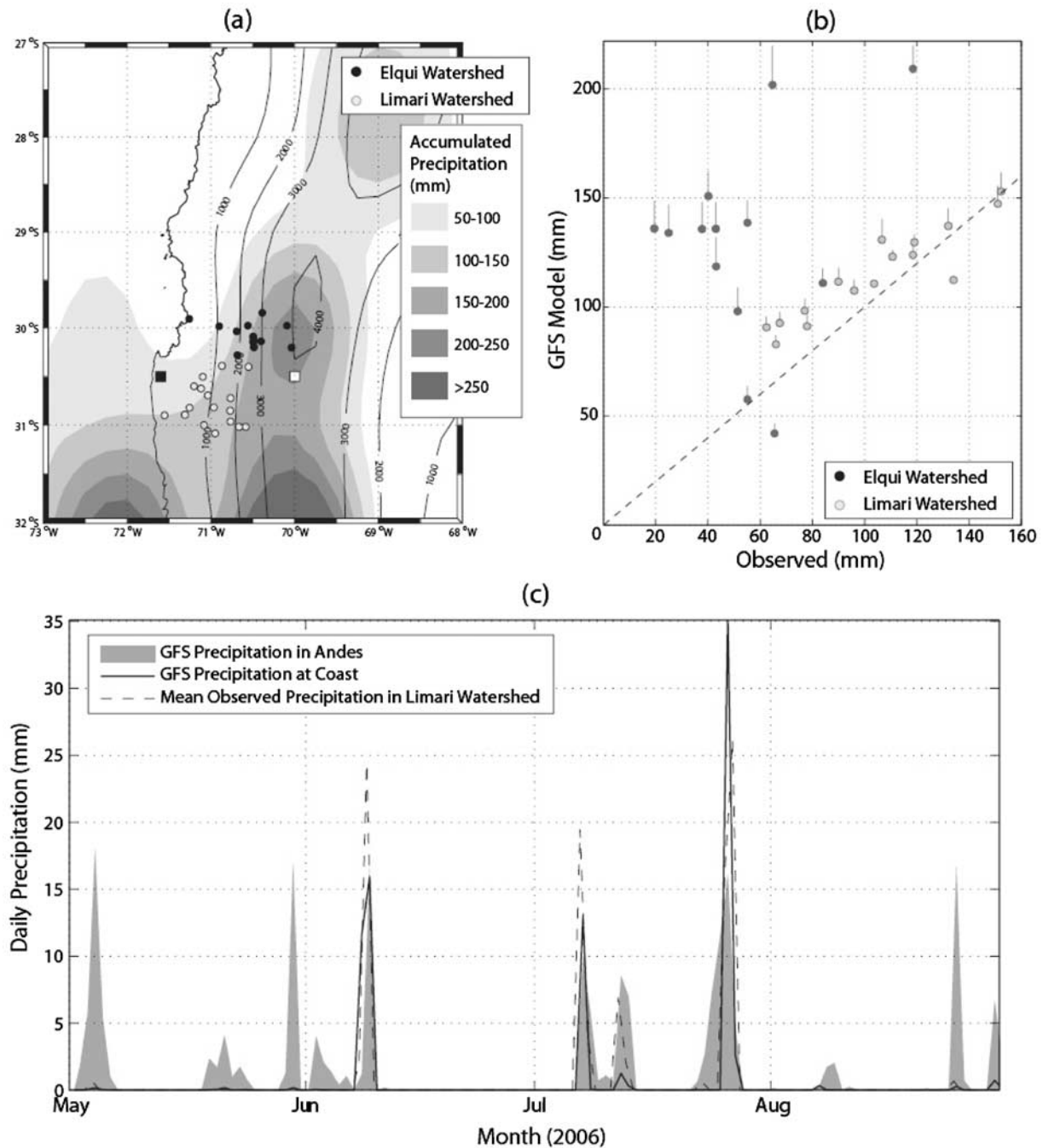


**Figure 11.** Spatial and temporal precipitation patterns from the GFS model for the period 1 May–30 September 2006. (a) Accumulated precipitation (shaded contours) and model topography (thin black contours). Black and gray circles identify precipitation gauge stations in the Elqui and Limari watersheds, respectively. The black square indicates the coastal location used in Figure 11c, and the white square indicates the Andean location. (b) Scatterplot comparing the mean observed cumulated precipitation (May–September) with the GFS model at sites in the Elqui (black) and Limari (gray) watersheds. The vertical bars represent the difference (always positive) between the height of the GFS model topography at each location and the actual station height ( $\Delta z$ ). Scale of the vertical bars, 1 mm (precipitation scale) = 50 m (elevation scale). The dashed line represents a perfect 1:1 ratio. (c) Time series of daily precipitation from the GFS model at a coastal (solid black line) and Andean (gray filled) location. The dashed line indicates the mean observed precipitation averaged over all stations in the Limari watershed.

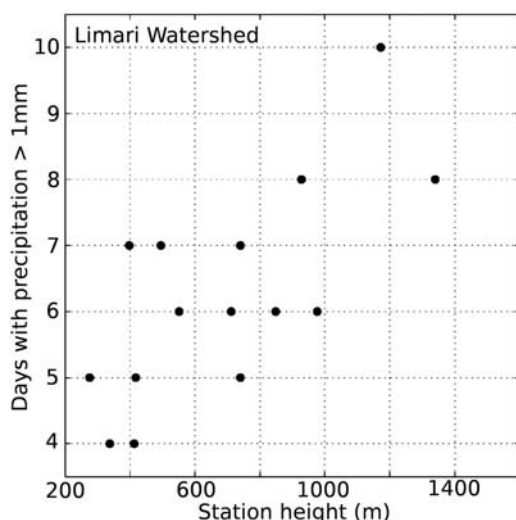


**Figure 12.** Variation of precipitation frequency with station altitude for sites in the Limari catchment for the period 1 May–30 September 2006.

inferring the characteristics of precipitation in these areas. Atmospheric models provide such an option, and in the following section we examine data from the GFS global weather model in order to see if it can tell us more about the spatial variation of precipitation in the Norte Chico and its elevation dependence. The WRF model was not considered because its precipitation field was simply too overestimated to be of any value.

[43] Figure 11a shows the GFS model accumulated precipitation for the winter (April–September) of 2006 along with the model's representation of topography. Clearly the spatial patterns are limited by the low model resolution, which is unable to represent the complex topographic structures (valleys, subridges) of the region. Nonetheless, the model clearly indicates that the precipitation increases with topographic height and the maximum closely follows the main ridge of the Andes. For example, at a coastal point near La Serena (black square) the winter precipitation is about 50 mm, while inland, near the (model) peak of the Cordillera, the model precipitation is 230 mm, an enhancement factor of about 5 times (Figure 11c).

[44] In Figure 11b available observed precipitation totals in the Limari and Elqui watersheds are compared with model values linearly interpolated to the station location. In the Limari Valley the comparison is very good, with a clear linear relationship between the model and observations. In the Elqui valley to the north, the comparison is somewhat poorer with the GFS precipitation much higher than the observations at many stations. However, this result is not unexpected given that the Elqui valley cuts more deeply into the Andes and most of the stations are well below the model heights at the same locations (note bar lengths on plots in Figure 11b). The mean model station height difference is 1000 m in this valley compared to 500 m in the Limari valley. If the strong increase in precipitation with topographic height implied by the model is real, large discrepancies are to be expected at the Elqui valley stations. The GFS precipitation was also compared with snowfall measurements made at the Pascua Lama mining

site (Figure 1) at 4000 m altitude near the main ridge of the Andes (not shown). The GFS winter precipitation at this location was 147 mm w.e., very close to the 126 mm w.e. that was actually observed. Although results at a single station are in no way conclusive, they are nonetheless encouraging and suggest that the GFS model may provide realistic estimates of high-altitude precipitation.

[45] The time series of daily precipitation provides further evidence of the quality of the GFS data and offers insight into the character of the orographic enhancement. First, the coastal precipitation rate shows significant correlation with the mean observed precipitation in the Limari watershed (mostly low-lying stations). Over the winter there were just 4 significant ( $>1$  mm/day) precipitation events, and each was predicted by the GFS model (with no false alarms). Occurrence of precipitation is well reproduced in high-altitude areas as we observed with available data at Pascua Lama mining site (not shown). Interestingly, the daily precipitation in the Andes during these events is similar to the lowland sites. The overall orographic enhancement is due to the fact that precipitation events occur more frequently and tend to last longer at the high altitude. Observational evidence of this behavior is presented in Figure 12, which shows that even for the relatively low altitude stations in the Limari watershed there is a detectable increase in the frequency of precipitation events as station altitude increases. We note that, with the exception of the Pascua Lama site, the model results at high elevations are essentially unverified. However, their good comparison with available low altitude data, along with the fact that increasing precipitation at high altitudes offers a good explanation for the high runoff coefficients derived from the discharge data (see section 5), does lend credibility to the idea that the high Andes experience more frequent precipitation than in the low lying coastal regions and alpine valleys.

[46] What is the cause of the additional precipitation events at high altitudes? While an in-depth investigation is beyond the scope of this study, it is of interest to briefly examine the meteorological conditions associated with them. Many studies in mountain ranges worldwide [e.g., Sinclair, 1994; Brasseur et al., 2002], including central Chile [Falvey and Garreaud, 2007] have shown precipitation to be strongly dependent on the wind speed (or nearly equivalently, the moisture flux) perpendicular to the axis of the orographic barrier, and the humidity of the upstream air mass. Figure 13 compares the composite vertical structure of the zonal wind and humidity using the GFS data interpolated to the coastal reference point (upwind) for days when precipitation  $> 1$  mm was predicted in the coast and Cordillera (*widespread rainfall*), in the Cordillera only and (for reference) on *days without rain*. A marked contrast between *days without rain* and those of *widespread rainfall* is seen in both the winds and humidity: rainy days showing (on average) positive cross-mountain winds at all levels (including the surface) and high humidity throughout especially in the lower troposphere. Days of isolated precipitation in the *Cordillera only* show a zonal wind profile nearly identical to that of the dry composite, with negligible winds below about 3000 m. However, the relative humidity is considerably higher than the *days without rain* composite, particularly at mid levels. It therefore appears that the

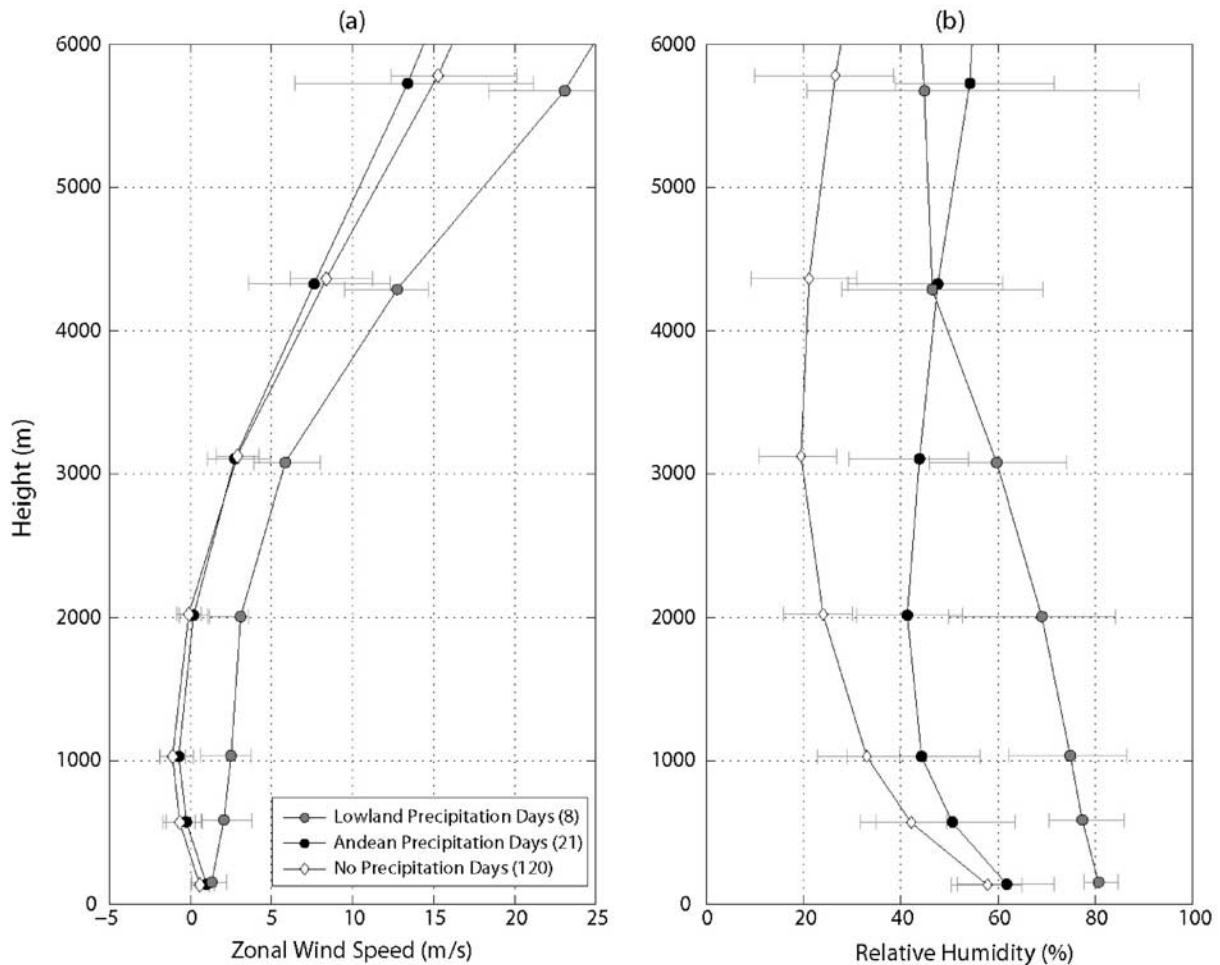


**Figure 13.** Composite vertical profiles. (left) Zonal wind speed and (right) relative humidity from the GFS model slightly upwind of La Serena ( $72^{\circ}\text{W}$ ,  $30^{\circ}\text{S}$ ). Gray circles show composites for days (8 in total) in which the model predicted precipitation of  $> 1$  mm at both the coastal and Andean location. Black circles are composites for days (21 in total) wherein daily precipitation of above 1 mm was only predicted in the Andes. The open diamonds show composites for the 120 remaining precipitation-free days. The error bars indicate the interquartile range of the composite members.

Andean precipitation events occur when the prevailing zonal flow is sufficiently moist to provoke grid scale condensation as the airstream crosses the Andes. A detailed analysis of the synoptic situations associated with such events is beyond the scope of this study. However, a preliminary inspection indicates that they are principally associated with the prefrontal air mass of precipitation events affecting regions to the south (some of which eventually cross the study area), or cutoff lows [Fuenzalida *et al.*, 2005; Garreaud and Fuenzalida, 2007] passing over the Norte Chico.

## 7. Water Budget Calculations

[47] In this section we provide a simple, quantitative examination of how inclusion of our estimates of glacial retreat, sublimation and orographic enhancement affects the water budget. We consider the Elqui, Limari and Choapa watersheds, and focus on their high-altitude subcatchments because (1) discharge is less affected by water extraction for irrigation in high-altitude areas and (2) these watersheds

present larger discrepancies between precipitation and discharge. Water budgets were computed with equation (1), assuming different values for precipitation. Sublimation was assumed to be  $80 \text{ mm a}^{-1}$ . Glaciers (including rock and debris covered glaciers) contribute to  $200 \text{ L s}^{-1}$  at La Laguna Embalse station (which is the maximum melting discharge computed in section 6.1.). However, glacier melt was neglected in other catchments because no precise inventory is available and few glaciers are found in the other catchments under study. Evaporation from soil and transpiration are assumed to be negligible because, above 3000 m asl, the catchments are steep, rock covered, and vegetation is totally absent except in the close vicinity of rivers. Simulation results with WRF also suggest that evaporation is absent without snow cover. Groundwater flow was also neglected due to a lack of data. The quality of the results is assessed by computing  $\varepsilon$  in equation (1). Considering a long period,  $\varepsilon$  should be close to nil.

[48] In our first experiment we interpolated precipitation measurements with the method presented in section 5. In the second experiment, precipitation from GFS was interpolated

**Table 3.** Results of Water Budget Computation<sup>a</sup>

Cuenca (ID number)	Specific Discharge (mm a <sup>-1</sup> )	Runoff Coefficient (%)	$\varepsilon$ With Precipitation Measurements (%)	$\varepsilon$ With Simple GFS Interpolation (%)	Precipitation Increase, GFS (%)	$\varepsilon$ With GFS Interpolation With Elevation (%)	Precipitation Increase, GFS + Elevation (%)
La Laguna Embalse (R10)	135	83	33	-29	151	-8	135
Cochiguaz En El Penon (R13)	135	130	85	7	201	-10	223
Est. Derecho En Alcoguz (R12)	124	76	35	12	118	-6	132
Hurtado En San Agustin (R17)	121	90	58	2	151	-24	174
Grande En Las Ramadas (R19)	328	99	24	62	63	66	58
Tascadero En Desembocadura (R20)	256	87	18	47	75	47	75
Cogoti En Fragueta (R21)	196	100	43	35	108	37	106
Combarbala En Ramadillas (R18)	409	180	65	70	90	62	105
Illapel En Las Burras (R33)	148	65	3	-1	103	-1	103
Chalinga En La Palmilla (R35)	483	193	65	61	107	62	106
Choapa En Cuncumen (R32)	304	106	33	10	125	10	125
Cuncumen Antes Bocatoma De Canales (R31)	164	57	-24	-32	105	-38	110
Mean	234	106	37	20	116	16	121

<sup>a</sup> $\varepsilon$  is expressed as a percentage of the specific discharge for different methods of interpolation for precipitation. Precipitation increase is the result of the ratio between the mean interpolated GFS precipitation and precipitation measurements (interpolated with the method presented in Figure 5).

linearly to a  $0.05^\circ \times 0.05^\circ$  grid and integrated over watersheds under study. Because important differences are observed between the height of the GFS model topography and actual height of local topography, we also examined (our third experiment) the impact of a topographic precipitation correction based on the following equation

$$P_{xy} = P(z) = \frac{P_i - P_j}{z_i - z_j} \cdot z + \frac{P_j z_i - P_i z_j}{z_i - z_j} \quad [\text{mm a}^{-1}] \quad (3)$$

[49] Where  $P_{xy}$  is precipitation at the point M of the grid of latitude ( $x$ ) and longitude ( $y$ ). ( $z$ ) is the elevation of this point in the SRTM (The Shuttle Radar Topography Mission) Digital Elevation Model;  $P_i$  and  $P_j$  are the precipitation of the two closest GFS grid points from M;  $z_i$ ,  $z_j$  are the elevation of these 2 points in the DEM.

[50] Results of the three experiments are displayed in Table 3. As discussed in section 5, water balances computed with measured precipitation and computed sublimation have a significant runoff excess, as  $\varepsilon$  is positive in almost all of the subcatchments considered. Inclusion of neglected terms of water loss due to evaporation and groundwater flow would induce an even higher runoff excess. Except in three catchments, the GFS precipitation is higher than the measured value (1.5 times larger in the La Laguna Embalse watershed, for example). As a result, the inclusion of GFS precipitation, leads to an improved water balance,  $\varepsilon$  being reduced in 8 of the 12 catchments. Performing the topographic precipitation correction has little impact on the results, indicating that the use of topography does not yield a significant improvement if physical processes of orographic precipitation are not precisely modeled.

[51] Uncertainty in our sublimation estimates and GFS precipitation is hard to define and expected to be rather high. Our sublimation estimates are reasonably low (about 80 mm w.e. a<sup>-1</sup>), and uncertainties could be as high as 50% given the differences we find between the WRF model and available field observations. We estimate that uncertainty in the glacier melt contribution is around 50–100%. However, because this contribution is relatively small (maximum 10%

of basin discharge), these uncertainties do not make a large impact on the water balance. Cumulated uncertainties on  $\varepsilon$  are about 60 mm w.e. a<sup>-1</sup> or 15–35% according to precipitation. Finally, GFS precipitation must be viewed with caution due to the low spatial resolution of the model and the limited time period that was considered (just 1 year of data). However, despite the large uncertainties, the use of GFS precipitation and our rough estimate of sublimation clearly improved that water balance. While our results are by no means definitive, they emphasize the importance both orographic precipitation enhancement and snow sublimation processes in the water balance of high-altitude areas of the Norte Chico region.

## 8. Conclusions

[52] Precipitation and discharge in the Norte Chico region have been studied over the 20th century. After a strong decrease before 1930, the mean precipitation has remained almost unchanged until today. Precipitation decrease induced a diminution in mean surface stream flows. Under the current precipitation and temperature regime, the cryosphere is not stable and retreats progressively inducing a non negligible contribution to high-altitude discharge (about 5–10% of La Laguna Embalse catchment, 3100 m asl), although this contribution becomes less important at lower altitudes. Even if glacier retreat accelerated over the last 10 years, water contribution from glaciers does not seem to have significantly increased during the last 50 years, because glacier surfaces significantly reduced at the same time.

[53] High-altitude areas are the main surface stream production areas of the Norte Chico region. Very high runoff coefficients (often > 100%) are observed for high-altitude catchments, leading to discrepancies between precipitation and discharge measurements in several catchments in the area. Even though the retreat of the cryosphere plays a significant role in some catchments, runoff deficit clearly suggests that precipitation should still increase above 3000 m asl and that sublimation processes

are rather weak during winter, allowing accumulated snow to be very effective in terms of surface stream production. Estimations by a regional circulation model and from past studies lead to a mean annual sublimation of about 80 mm  $a^{-1}$  at 4000 m asl. Results from the GFS atmospheric model indicate that maximum annual precipitation occurs near the main ridge of the Andes, mainly because precipitation events at high altitudes occur more frequently and tend to last longer than those in low lying areas. The GFS precipitation at 4000 m asl is almost 1.5 times larger than measurements of the highest available rain gauges. Inclusion of GFS precipitation, along with the estimate of sublimation, in simple water balance calculations leads to better closure of the water budget for most high-altitude catchments.

[54] Future work will be to improve precipitation regionalization methods in order to resolve the effects of local topography. Because precipitation events at high altitudes are not always connected with those at low altitude, estimation of precipitation at high altitudes from the simple extrapolation of low altitude measurements is likely to be erroneous and application of regional circulation models based on physical equations is recommended. However, the fact that current generation mesoscale models (such as WRF) significantly overestimate the precipitation in the Andes indicates that this may be a challenging task. Once reliable precipitation fields have been obtained an integrated modeling approach, involving more sophisticated mass balance and snowpack modeling [e.g., Lehning et al., 2006], will be required to better understand the hydrology of the Norte Chico. Such modeling efforts will clearly need to be complemented by targeted field measurements aimed at filling in the substantial gaps in the regions observational networks.

[55] **Acknowledgments.** We are particularly grateful to DGA-Chile, DMC for granting access to precipitation and runoff data. We also particularly thank three anonymous reviewers and Michael Lehning for their very helpful comments which greatly improved the manuscript. Vincent Favier was supported by Fondecyt project N° 3070056. Mark Falvey was supported by CONICYT project ACT-19.

## References

- Aceituno, P. (1988), On the functioning of the Southern Oscillation in the South American Sector: part I. Surface climate, *Mon. Weather Rev.*, *116*, 505–524.
- Alfaro, C., and C. Honores (2001), Análisis de la Disponibilidad del Recurso Hídrico Superficial en Cauces Controlados de las Cuencas de los Ríos Elqui, Limarí y Choapa, Master degree thesis, 204 pp., Univ. of La Serena, La Serena, Chile.
- Arakawa, A., and W. H. Shubert (1974), Interaction of a cumulus ensemble with the large-scale environment: part I, *J. Atmos. Sci.*, *31*, 674–704.
- Begert, M. (1999), Klimatologische untersuchungen in der weiteren umgebung des Cerro Tapado, Norte Chico, Chile, Master degree thesis, Univ. of Berne, Berne, Switzerland.
- Bergeron, V., C. Berger, and M. D. Betterton (2006), Controlled irradiative formation of penitents, *Phys. Rev. Lett.*, *96*, 098502, doi: 10.1103/PhysRevLett.96.098502.
- Bintanja, R., and R. Van den Broeke (1995), The surface energy balance of Antarctic snow and blue ice, *J. Appl. Meteorol.*, *34*(4), 902–926.
- Brasseur, O., H. Gallée, D. Creutin, J. T. Lebel, and P. Marbaix (2002), High resolution simulations of precipitation over the Alps with the perspective of coupling to hydrological models, *Adv. Global Change Res.*, *10*, 75–100.
- Brenning, A. (2005), Climatic and geomorphological controls of rock glaciers in the Andes of central Chile: Combining statistical modelling and field mapping, Ph.D. dissertation, Mathematisch-Naturwissenschaftliche Fakultät II, Humboldt-Universität zu Berlin, Berlin, urn:nbn:de:kobv:11-10049648.
- Chen, F., and J. Dudhia (2001), Coupling an advanced land surface-hydrology model with the Penn State-NCAR MM5 modeling system: part I. Model implementation and sensitivity, *Mon. Weather Rev.*, *129*(4), 569–585.
- Chou, M.-D., and M. J. Suarez (1994), An efficient thermal infrared radiation parameterization for use in general circulation models, *NASA Tech. Memo. 104606*, vol. 3, 102 pp.
- Comisión Nacional de Medio Ambiente (CONAMA) (1999), *Primera Comunicación Nacional Bajo la Convención Marco de las Naciones Unidas Sobre el Cambio Climático*, CONAMA report, Santiago, Chile.
- Comisión Nacional de Medio Ambiente (CONAMA) (2007), *Resultados Proyecto Estudio de la Variabilidad Climática en Chile para el Siglo XXI*, by DGF/UCH for CONAMA, CONAMA report, Santiago, Chile.
- Corripio, J. G., and R. S. Purves (2005), Surface energy balance of high altitude glaciers in the central Andes: The effect of snow penitents, in *Climate and Hydrology in Mountain Areas*, edited by C. de Jong, D. Collins, and R. Ranzi, pp. 15–27, John Wiley, London, U.K.
- Escobar, F., and P. Aceituno (1998), Influencia del fenómeno ENSO sobre la precipitación nival en el sector andino de Chile Central, durante el invierno austral, *Bull. Inst. Fr. Etudes Andines*, *27*(3), 753–759.
- Falvey, M., and R. Garreaud (2007), Wintertime precipitation episodes in Central Chile: Associated meteorological conditions and orographic influences, *J. Hydrometeorol.*, *8*, 171–193.
- Favier, V., P. Wagnon, J. P. Chazarin, L. Maisincho, and A. Coudrain (2004), One-year measurements of surface heat budget on the ablation zone of Antizana Glacier 15, Ecuadorian Andes, *J. Geophys. Res.*, *109*, D18105, doi:10.1029/2003JD004359.
- Fuenzalida, H. A., R. Sanchez, and R. D. Garreaud (2005), A climatology of cutoff lows in the Southern Hemisphere, *J. Geophys. Res.*, *110*, D18101, doi:10.1029/2005JD005934.
- Garin, C. (1987), Inventario de Glaciares de los Andes Chilenos desde los 18° a los 32° de latitud sur, *Rev. Geogr. Norte Grande*, *14*, 35–48.
- Garreaud, R., and H. Fuenzalida (2007), The influence of the Andes on cutoff lows: A modeling study, *Mon. Weather Rev.*, *135*, 1596–1613.
- Garreaud, R., J. Rutllant, and H. Fuenzalida (2002), Coastal lows in north-central Chile: Mean structure and evolution, *Mon. Weather Rev.*, *130*, 75–88.
- Ginot, P., C. Kull, M. Schwikowski, U. Schotterer, B. Pouyaud, and H. W. Gäggeler (2001), Effects of post-depositional processes on snow composition of a subtropical glacier (Cerro Tapado Chilean Andes), *J. Geophys. Res.*, *106*, 32,375–32,386.
- Ginot, P., C. Kull, U. Schotterer, M. Schwikowski, and H. W. Gäggeler (2006), Glacier mass balance reconstruction by sublimation induced enrichment of chemical species on Cerro Tapado (Chilean Andes), *Clim. Past*, *2*, 21–30.
- Hall, D. K., G. A. Riggs, and V. V. Salomonson (2006), MODIS snow and sea ice products, in *Earth Science Satellite Remote Sensing-Volume I: Science and Instruments*, edited by J. J. Qu et al., pp. 154–181, Springer, New York.
- Hong, S.-Y., and H.-L. Pan (1996), Nonlocal boundary layer vertical diffusion in a medium-range forecast model, *Mon. Weather Rev.*, *124*, 2322–2339.
- Hong, S.-Y., H.-M. H. Juang, and Q. Zhao (1998), Implementation of prognostic cloud scheme for a regional spectral model, *Mon. Weather Rev.*, *126*, 2621–2639.
- Intergovernmental Panel on Climate Change (IPCC) (2007), *IPCC Fourth Assessment Report, Working Group I Report (WGI): Climate Change 2007: The Physical Science Basis*, 996 pp., Cambridge Univ. Press, Cambridge.
- Kain, J. S., and J. M. Fritsch (1993), Convective parameterization for mesoscale models: The Kain-Fritsch scheme. The representation of cumulus convection in numerical models, *Meteor. Monogr.*, vol. 46, pp. 165–170, Am. Meteorol. Soc.
- Kalnay, E., M. Kanamitsu, and W. E. Baker (1990), Global numerical weather prediction at the National Meteorological Center, *Bull. Am. Meteorol. Soc.*, *71*, 1410–1428.
- Kalthoff, N., I. Bischoff-Gauss, M. Fiebig-Wittmaack, F. Fiedler, J. Thürauf, J. E. Novoa, C. Pizarro, L. Gallardo, and R. Rondanelli (2002), Mesoscale wind regimes in Chile at 30°S, *J. Appl. Meteorol.*, *41*, 953–970.
- Kalthoff, N., M. Fiebig-Wittmaack, C. Meißner, M. Kohler, M. Uriarte, I. Bischoff-Gauß, and E. González (2006), The energy balance, evapotranspiration and nocturnal dew deposition of an arid valley in the Andes, *J. Arid Environ.*, *65*, 420–443.
- Kanamitsu, M. (1989), Description of the NMC global data assimilation and forecast system, *Weather Forecast.*, *4*, 335–342.

- Khodayar, P., N. Kalthoff, M. Fiebig-Wittmaack, and M. Kohler (2007), Evolution of the atmospheric boundary layer structure of an arid valley, *Meteorol. Atmos. Phys.*, *271*, 227–243.
- Kull, C., M. Grosjean, and H. Veit (2002), Modeling modern and late Pleistocene Glacio-climatological conditions in the north Chilean Andes (29–30°S), *Clim. Change*, *52*, 359–381.
- Krainer, K., and W. Mostler (2002), Hydrology of active rock glaciers: Examples from the Austrian Alps, *Arct. Antarct. Alp. Res.*, *34*(2), 142–149, doi:10.2307/1552465.
- Lehning, M., I. Völksch, D. Gustafsson, T. A. Nguyen, M. Stähli, and M. Zappa (2006), ALPINE3D: A detailed model of mountain surface processes and its application to snow hydrology, *Hydrol. Processes*, *20*, 2111–2128.
- Leiva, J. C. (1999), Recent fluctuations of the Argentinian glaciers, *Global Planet. Change*, *22*, 169–177.
- Le Quesne, C., D. W. Stahle, M. K. Cleaveland, M. D. Therrell, J. C. Aravena, and J. Barichivich (2006), Ancient austrocedrus tree-ring chronologies used to reconstruct central Chile precipitation variability from a.d. 1200 to 2000, *J. Clim.*, *19*(22), 5731–5744.
- Lliboutry, L. (1954), The origin of penitents, *J. Glaciol.*, *2*, 331–338.
- Luebert, F., and P. Plissock (2006), *Sinopsis Bioclimática y Vegetacional de Chile*, Editorial Universitaria, Univ. de Chile, Santiago, Chile.
- Mark, B. G., and J. M. McKenzie (2007), Tracing increasing tropical Andean glacier melt with stable isotopes in water, *Environ. Sci. Technol.*, *41*(20), 6955–6960.
- Mark, B. G., and G. O. Seltzer (2003), Tropical glacial meltwater contribution to stream discharge: A case study in the Cordillera Blanca, Perú, *J. Glaciol.*, *49*(165), 271–281.
- Messerli, B., C. Ammann, M. Geyh, M. Grosjean, B. Jenny, K. Kammer, and M. Vuille (1996), Current precipitation, Late Pleistocene snow line and lake level changes in the Atacama Altiplano (18°S–28°/29°S), *Bamberg Geogr. Schr.*, *15*, 17–35.
- Ministerio de Obras Públicas–Dirección General de Aguas (MOP-DGA) (1984), Balance hidrológico nacional, Regiones III y IV, by IPLA Ingenieros Consultores for DGA MOP-DGA report, Santiago, Chile.
- Mlawer, E. J., S. J. Taubman, P. D. Brown, M. J. Iacono, and S. A. Clough (1997), Radiative transfer for inhomogeneous atmosphere: RRTM, a validated correlated-k model for the longwave, *J. Geophys. Res.*, *102*, 16,663–16,682.
- Novoa, J. E. (2006), Cambio Climático del Ecosistema Semiárido Transicional en Chile (IV Región de Coquimbo), mediante Análisis de Tendencia de Caudales Naturales, Cambio Climático del Ecosistema, Ph.D. thesis, 177 pp., Univ. Nacional de Cuyo, Cuyo.
- Novoa, J. E., R. Castillo, and K. Debonis (1995), Tendencia de cambio climático mediante análisis de caudales naturales: Cuenca del río La Laguna (Chile Semiárido), in *Anales de la Sociedad Chilena de Ciencias Geográficas*, pp. 279–288, Univ. Austral de Chile, Valdivia, Chile.
- Novoa, J. E., R. Castillo, and J. M. Viada (1996), Tendencia de cambio climático mediante análisis de caudales naturales: Cuenca del río Claro (Chile Semiárido), in *Anales de la Sociedad Chilena de Ciencias Geográficas*, pp. 47–56, Univ. de La Serena, La Serena, Chile.
- Pouyaud, B., M. Zapata, J. Yerren, J. Gomez, G. Rosas, W. Suarez, and P. Ribstein (2005), Avenir des ressources en eau glaciaire de la Cordillère Blanche, *Hydrol. Sci. J.*, *50*(6), 999–1022.
- Rivera, A., G. Casassa, C. Acuña, and H. Lange (2000), Variaciones de glaciares en Chile, *Invest. Geogr. Chile*, *34*, 29–60.
- Rivera, A., C. Acuña, G. Casassa, and F. Bown (2002), Use of remote sensing and field data to estimate the contribution of Chilean glaciers to sea level rise, *Ann. Glaciol.*, *34*, 367–372.
- Rojas, M. (2006), Multiply nested regional climate simulation for southern South America: Sensitivity to model resolution, *Mon. Weather Rev.*, *134*(8), 2208–2223.
- Rutllant, J., and H. Fuenzalida (1991), Synoptic aspects of central rainfall variability associated with the Southern Oscillation, *Int. Climatol. J.*, *11*, 63–76.
- Santibañez, F. (1997), Tendencias seculares de la precipitación en Chile, in *Diagnóstico Climático de la Desertificación en Chile*, edited by G. Soto and F. Ulloa, CONAF, La Serena, Chile.
- Sinclair, M. R. (1994), A diagnostic model for estimating orographic precipitation, *J. Appl. Meteorol.*, *33*, 1163–1175.
- Skamarock, W. C., and J. B. Klemp (2007), A time-split nonhydrostatic atmospheric model for research and NWP applications, *J. Comput. Phys.*, *227*, 3465–3485.
- Stichler, W., U. Schotterer, K. Fröhlich, P. Ginot, C. Kull, H. W. Gäggeler, and B. Pouyaud (2001), The influence of sublimation on stable isotope records from high altitude glaciers in the tropical Andes, *J. Geophys. Res.*, *106*, 22,613–22,621.
- Squeo, F. A., M. Holmgren, M. Jiménez, L. Albán, J. Reyes, and J. R. Gutiérrez (2007), Tree establishment along an ENSO experimental gradient in the Atacama desert, *J. Veg. Sci.*, *18*, 195–202.
- Vuille, M., and C. Ammann (1997), Regional snowfall patterns in the high arid Andes, *Clim. Change*, *36*, 413–423.
- Vuille, M., and F. Keimig (2004), Interannual variability of summertime convective cloudiness and precipitation in the central Andes derived from ISCCP-B3 data, *J. Clim.*, *17*, 3334–3348.
- Vuille, M., and J. P. Milane (2007), High-latitude forcing of regional aridification along the subtropical west coast of South America, *Geophys. Res. Lett.*, *34*, L23703, doi:10.1029/2007GL031899.
- Wagnon, P., P. Ribstein, B. Francou, and B. Pouyaud (1999), Annual cycle of energy balance of Zongo Glacier, Cordillera Real, Bolivia, *J. Geophys. Res.*, *104*, 3907–3923.
- Wagnon, P., J. E. Sicart, E. Berthier, and J. P. Chazarin (2003), Wintertime high altitude surface energy balance of a Bolivian glacier, Illimani, 6340 m above sea level (a.s.l.), *J. Geophys. Res.*, *108*(D6), 4177, doi:10.1029/2002JD002088.
- Zech, R., C. Kull, and H. Veit (2006), Late Quaternary glacial history in the Encierro Valley, northern Chile (29°S), deduced from 10Be surface exposure dating, *Paleogeogr. Paleoclim. Paleocol.*, *234*, 277–286.
- Zhao, Q. Y., and F. H. Carr (1997), A prognostic cloud scheme for operational NWP models, *Mon. Weather Rev.*, *125*, 1931–1953.

M. Falvey, Departamento de Geofísica, Universidad de Chile, Blanco Encalada 2002, Santiago, Chile. (falvey@dgf.uchile.cl)

V. Favier, Laboratoire de Glaciologie et de Géophysique de l'Environnement, 54, rue Molière, BP 96, 38402 Saint Martin d'Hères Cedex, France. (vifavier@gmail.com)

D. López and A. Rabatel, Laboratorio de Glaciología, CEAZA, Benavente 980, casilla 599, La Serena, Chile. (david.lopez@ceaza.cl; rabatelo@ceaza.cl)

E. Praderio, Division Hydraulique de Rivière, Hydrétudes, 815, Route de Champ Farçon, 74370 Argonay, France. (estelpra@hotmail.com)